# PETROGRAPHIC STUDY OF SEVEN SAMPLES RECOVERED FROM THE NAHANNI FORMATION AT WELL LOCATION B.A. TEXACO ARROWHEAD B-76 300/B-76-6030-12245/0

Northwest Territories Geological Survey
Work Order No. 20A20311

March, 2020

**AGAT Laboratories**
3801 – 21st Street N.E.
Calgary, Alberta T2E 6T5

AGAT Laboratories

SERVICE BEYOND ANALYSIS

## TABLE OF CONTENTS

## EXECUTIVE SUMMARY

The purpose of this study is to describe the observed lithological characteristics, associated reservoir quality and fluid sensitivity of seven petrographic samples collected from the Nahanni Formation at well location B.A. Texaco Arrowhead B-76 300/B-76-6030-12245/0. Petrographic analyses and interpretations are based on the observation of thin section samples generated from core and SEM samples, while Bulk XRD analyses (see **Figure 2** in Tables and Figures section of the report) were also completed for five (5) samples to confirm mineralogy. An overview of general sample information can be found below within **Table A:**

| **Sample ID (*)** | **Depth (ft/m)** | **Formation** | **Rock Classification** | **Analysis (*)** | **RQ (*)** |
|---|---|---|---|---|---|
| **Location: B.A. Texaco Arrowhead B-76 300/B-76-6030-12245/0** | | | | | |
| T21/S21 | 8923.50/2719.88 | Nahanni | Dolostone | TS; SEM | P |
| T20/X39/S20 | 8927.00/2720.95 | Nahanni | Limestone (Grainstone) | TS; XRD; SEM | P |
| T19/X38/S19 | 8946.30/2726.83 | Nahanni | Limestone (Wackestone) | TS; XRD; SEM | P |
| T18/X37/S18/P11 | 8963.25/2732.00 | Nahanni | Dolostone | TS; XRD; SEM; RC | P |
| T17/X36/S17/P10 | 8988.20/2739.60 | Nahanni | Dolostone | TS; XRD; SEM; RCA | P |
| X35/P9 | 8997.00/2742.29 | Nahanni | NA | XRD; RCA | P |
| T16/S16/P8 | 9000.40/2743.32 | Nahanni | Limestone (Mudstone) | TS; SEM; RCA | P |
| T15/S15/P7 | 9006.00/2745.03 | Nahanni | Limestone (Wackestone-Mudstone) | TS; SEM; RCA | P |

**(*) TS: Detailed thin section analysis with Images; XRD: Bulk X-Ray Analysis; SEM: Scanning Electron Microscope analysis with images; RCA: Routine Core Analysis**

**Sample ID: T – thin section sample; X – XRD; S – SEM sample; P – RCA**

**(*) RQ -Reservoir Quality: VP – Very Poor; P- Poor; M – Moderate; G- Good**

The total seven samples represent Middle Devonian Nahanni Formation.

To describe the original texture of the rocks the modified Dunham (1962) classifications for carbonate rocks was used (see the figure below).

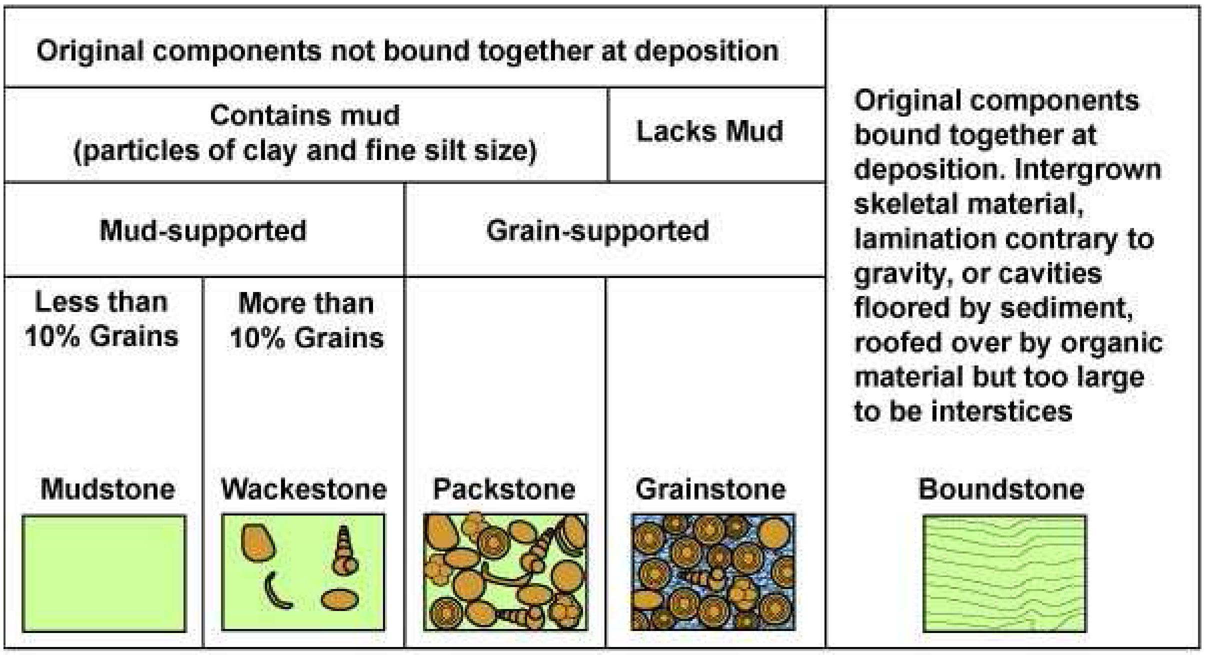


*C. G. St. C. Kendall, 2005 (after Dunham, 1962, AAPG Memoir 1)*

Based on the mineralogy, three of the study sample were classified as dolostone [T21, T18, and T17], while the other four samples are limestones. The limestone samples show grainstone (T20), wackestone (T19), mudstone (T16), and wackestone to mudstone (T15) texture. Dolostone samples are coarse to very coarse crystalline and do not show any remnants of the original texture of the precursor rock.

<u>Limestone samples.</u>

The mineralogy of the limestone sample is dominated by calcite (88% to 99% of the total rock volume), while dolomite (5% to 10%), pyrite (trace to 1%), clays and organic matter (trace to 2%), pyrobitumen (1% - only in sample T20), and trace quartz (samples T19 and T15) are the other minerals. The framework components (allochems) include only bioclast fragments such as crinoids, corals, stromatoporoid, mollusks, brachiopod, ostracods, plus also some highly fragmented and impossible to identify indistinct bioclast fragments. There are no carbonate clasts (ooids, peloids or intraclasts) observed in any of the limestone sample. Non-carbonate allochems were identified as phosphatic ostracode shell fragments and were only detected in trace amounts in sample T19.

Orthochems are dominated by micritic lime-mud. Micrite (microcrystalline calcite) consists of 1 to 4 μm crystals and forms as an inorganic precipitate or through breakdown of coarser carbonate grains. Micrite is produced within the basin of deposition and shows little or no evidence of significant transport (Folk, 1959). In the Wentworth division of the carbonate sediments that is mentioned in the following chapters of the report, micrite corresponds to aphanocrystalline size of the crystals. The distribution of matrix varies between the samples that belong to a particular lithology type. The more abundant matrix was observed in mudstone (T16), with lesser amounts of matrix in the wackestone and wackestone to mudstone samples (T19, and T15 respectively), while grainstone sample T20 contains only very minor (2%) amounts of micrite. During neomorphism[1] some of the micrite matrix has been recrystallized to microspar (crystal size from 5 to 20 μm) or pseudospar (crystal size larger than 30 to 50 μm). Microspar and pseudospar comprise elongated crystals with irregular and sutured boundaries that usually display patchy distribution and grades into a typical micrite. Note that the recrystallization of primary lime-mud to coarser crystalline micro- or pseudospar slightly reduces the amount micro-intercrystalline porosity. Besides the micrite and micro- or pseudospar, trace to minor amounts of clays and organic material were also point counted as a part of the matrix. The total pore filling cements range from 1% (grainstone sample T20) up to 15% (sample T15) and include mainly calcite spar (10%), with minor non-ferroan dolomite (1% to 5%), pyrobitumen (1% - only in sample T20), plus trace pyrite. Replacement minerals include trace to minor pyrite, plus trace authigenic quartz (sample T19).

There is no visible porosity in these four limestone samples. The main porosity plugging factors for wackestone, mudstone, and wackestone-mudstone samples is the abundance of calcite

[1] Diagenetic transformation of one mineral and itself or a polymorph, whether the new crystals are larger, smaller or differ in shape from the previous ones or represent new mineral species. Includes both inversion and recrystallization. (Folk, 1965).

micrite, which has locally recrystallized to tight mosaic microspar, plus the cementation (mainly of natural fractures) by calcite spar, coarse crystalline dolomite, plus trace pyrite. In the grainstone sample T20, the compaction (both mechanical and chemical), followed by the precipitation of syntaxial overgrowths on the crinoids plates plays the main role in destruction of the primary interparticle porosity.

Reservoir quality for the wackestone, mudstone, and wackestone-mudstone samples is mainly controlled by depositional environment (i.e. sediment texture, abundance and distribution of framework grains such as bioclasts fragments and non-skeletal carbonate grains, abundance and distribution of the matrix, etc.,) and to lesser extent by diagenesis (i.e. mineral diagenesis, recrystallization of micrite to microspar, compaction, and cementation). Reservoir quality is considered to be poor for these three samples.

For the limestone-grainstone sample T20, the reservoir potential is almost equally controlled by depositional environment (i.e. original sediment texture with abundance of the bioclasts) and by diagenetic events (i.e. mechanical and chemical compaction, precipitation of the framework sustaining cements such as syntaxial overgrowths, residual hydrocarbon etc.). Reservoir quality of the grainstone is also considered to be poor due to lack of visible porosity.

Dolostone samples

All three dolostone samples comprise primarily dolomite (93% to 97%), plus insignificant amounts of calcite (trace to 2%), quartz (trace to 4%), pyrite (trace to 2%), pyrobitumen (1% to 2%), plus clays and organics (trace to 1%).

The bulk of dolomite in these samples is coarse to very coarse crystalline replacement dolomite that locally shows sweeping extinction (saddle or baroque dolomite). Dolomite has replaced both allochems and orthochems. Pervasive dolomitization was overall nonmimic and the original texture of the precursor limestone has been destroyed. Only in sample T21 minor amounts of totally dolomitized indistinct bioclast fragments (possibly stromatoporoid fragments) can be observed (see Figure 1.2). Trace amount of dolomite cement that occludes micro-vuggy pores was spotted in samples T18 and T17. Other minerals that act as porosity plugging cements include authigenic quartz, pyrobitumen, plus pyrite.

The visible porosity in these three samples include trace to minor micro-vuggy (samples T18 and T17) and intercrystalline pores (sample T21). The porosity reducing factors include precipitation of calcite spar cement, which is a part of de-dolomitization process, authigenic quartz, pyrobitumen, and pyrite.

Reservoir quality is controlled mainly by diagenetic events [i.e. dolomitization, dissolution, compaction, cementation (mostly euhedral dolomite) and pyrobitumen] and to a lesser extent the depositional environment (i.e. the original carbonate texture influences dolomite crystal size which correlates to the size and efficiency of the intercrystalline and micro-vuggy pores). Reservoir quality for these three dolostone samples is assessed as poor.

Detailed mineralogical composition of each of the study samples are summarized in the tables that can be find in the 'RESULTS' chapter of this report, plus in the **Petrographic Summary Table 1** that is located in the **Tables and Figures** section of the report. Following the tabulated data there are this section and SEM images (with descriptions) that show specific features of the samples.

The reservoir quality rating is based solely on the thin section examination. The following table is the summary of the reservoir quality at the study locations.

## NAHANNI Formation

| Sample ID | Depth (ft & m) | Total Micrite (%) | Total Cement/ Replacement (%) | Total Porosity (%) | | | | | | Main Porosity controlling factors (*) | RQ(*) |
|---|---|---|---|---|---|---|---|---|---|---|---|
| | | | | IP | Int. | Ixl | Mv | Fr | M | | |
| **Location: B.A. Texaco Arrowhead B-76 300/B-76-6030-12245/0** | | | | | | | | | | | |
| T21 | 8923.50ft 2719.88m | - | 97 | - | - | TR | - | - | - | Mic; Dol; Com; Cc; C; OM; Qc; Py | P |
| T20 | 8927.00ft 2720.95m | 2 | TR | - | - | - | - | - | - | Com; Ov; Mic; C; S; OM; Py | P |
| T19 | 8946.30ft 2726.83m | 39 | 1 | - | - | - | - | - | - | Mic; Cc; Ms; Com; Py; C; Qc | P |
| T18 | 8963.25ft 2732.00m | - | 100 | - | - | TR | TR | - | - | Mic; Dol; Py; OM; Qc; Com; Dis | P |
| T17 | 8988.20ft 2739.60m | - | 100 | - | - | 1 | 3 | - | - | Mic; Dol; Qc; Com; Dis; OM; Cc; Py; C | P |
| T16 | 9000.40ft 2743.32m | 74 | 16 | - | - | - | - | - | - | Mic; Cc; Dol; Ms; Dc; Py; C | P |
| T15 | 9006.00ft 2745.03m | 41 | 21 | - | - | - | - | - | - | Mic; Ms; Dc; Dol; C; Py | P |

**Porosity value (%):** **IP** – interparticle porosity; **Int** – intraparticle; **Ixl** – intercrystalline; **Mv** – micro-vuggy; **Fr** – fracture porosity; **M** – micro-intercrystalline porosity
**Main Porosity controlling factors:** **Com –** compaction (mechanical and chemical)**; Dol** – dolomitization; **Mic** – micrite (calcite or dolomite) and/or micritization; **Ms** – micro- and/or pseudospar; Cc – calcite cement (druse and spar); **Dc** – dolomite cement**; C** – clays and organics; **Qc** – quartz/chert cement; **Ov** – crinoid overgrowths; **Py** – pyrite (replacement and/or cement); **OM** – organic matter/pyrobitumen; **Dis** – dissolution; **F** – fabric: [**CC** – concavo-convex orthochem contacts; S – sutured orthochem contacts]
**RQ (*) - reservoir quality: VP –** very poor; **P –** poor; **M –** moderate; **G** - good

Reservoir problems for the samples recovered from the Nahanni Formation at the B.A. Texaco Arrowhead B-76 300/B-76-6030-12245/0 location may include the following: **(1)** rare and small sizes of intercrystalline and micro-vuggy pores, plus overall poor interconnectivity between pores could restrict the flow of hydrocarbons, **(2)** hydrochloric acid (HCl) treatment of this reservoir has the potential to loosen carbonate fines (calcite micrite) that could migrate and block pore throats, plus cause fabric collapse, **(3)** the sensitivity of calcium carbonate to hydrofluoric acid (HF) in regard to precipitation of calcium fluoride scales, (4) Pore lining pyrobitumen (especially in dolostone samples) may react with hydrochloric acid (HCl) to create sludges or viscous emulsions, which can restrict permeability potential. Both sludges and emulsions may be removed by using appropriate surfactants (surface active agents), which reduce interfacial and surface tension and result in a more miscible mixture of oil and water (acid). Any drilling, completion or workover must ensure the fluid acid compatibility with the formation pyrobitumen.

## METHODS

### Petrographic Microscopy

The thin section samples were cut from unclean core samples, and then impregnated with blue epoxy, polished and mounted onto a glass slide. After drying of the epoxy the samples were ground down to a total thin section thickness of 30µm. One half of each thin section was then stained with a combination of Alizarin Red (for calcite) and potassium ferricyanide (for ferroan carbonate) to highlight carbonate mineralogy, while the other half remained unstained. The dual carbonate stain helps to differentiate the carbonate components within the samples, and affects them as follows: calcite appear pink to red-brown, ferroan calcite shows mauve to blue, ferroan dolomite colors vary from pale blue to turquoise, while non-ferroan dolomite remains unstained. Finally a second glass slide was glued on the samples to protect the polished surface. The prepared thin sections were point counted (see the **Petrographic Summary Table 1**). The thin sections were examined in plain and cross polarized light conditions and photomicrographs taken at various magnifications (x12.5ppl; x25ppl; x50ppl, and x100ppl) to document structure, porosity, composition and nature of optically resolvable grains and matrix. To determine original texture of dolostone samples, the 'white card' technique has been used. Each sample has been described separately and the important features of it that includes framework mineralogy, diagenetic minerals and cements, textures, grain size range and average, porosity, etc., and the results are provided in the tabulated format. Annotated images of the thin sections with descriptions show the important aspects that were observed during the thin section examination. These images are placed after the tabulated data.

### SEM Analysis

A representative portion of each sample was adhered onto an aluminum stub specimen mount. The stubs were then sputter-coated with a conductive gold-palladium alloy for detailed Scanning Electron Microscopy (SEM) analysis and imaging. SEM analysis is useful in identifying lithological characteristics such as pore types, framework mineralogy, clay and cement composition, in addition to the potential deportment of clay constituents in relation to pore spaces and pore throats. Energy dispersive X-ray (EDX) was also used in conjunction with SEM observation in order to determine the elemental composition of the observed clay minerals and overall mineralogy.

Bulk XRD Analysis

Sample Preparation: Each sample, consisting of rock fragments, is manually crushed carefully using a mortar and pestle to reduce the size of the fragments. The sample is then ground with a vibratory disc mill (RS200; Retsch) to further reduce crystallite sizes. Finally, the sample is micronized using a planetary ball mill (PQN04; Across International) and scanned for X-ray diffraction analysis.

X-Ray Data Collection and Analysis:
Diffractometer Name: Bruker D4 Endeavor XRD with a Lynx-Eye detector
Instrumental Parameters: Radiation Source – Cobalt (Co)
Generator settings - 40 mA, 35 kV
Start position [°2θ] - 4
End position [°2θ] - 80
Step size [°2θ] - 0.02
Scan step time [s] - 1
Data Analysis: ICDD PDF-4 Mineral 2020 powder diffraction database
X'PERT HighScore Software for mineral identification
TOPAS Software for quantitative phase analysis
Detection Limit: 0.1 – 0.5 % depending on the type and nature of sample

Quantitative Mineral Phase Analysis: Using the HighScore program, the different mineral phases of the XRD patterns are identified. Once the mineral phases are identified, Rietveld refinements are performed by importing the XRD trace pattern into TOPAS 5. This program (TOPAS 5) is used for Rietveld analysis to quantify the mineralogy. The quantitative mineral phases of all samples are given in **Table 2**. The refined diffractograms and **Table 2** are placed in the **Tables and Figures** section of this report.

Grain sizes:

The scale for authigenic constituents in carbonates follows the Wentworth division, which is the most useful for dolomites, where transported particles are usually obliterated by replacement and crystal size is one of the few describable characteristic. The carbonate crystal sizes ranges are as follows: very fine crystalline (4 to 16µm), fine (16 to 62 µm), medium (62 to 250 µm), coarse (250-1000 µm), and very coarse crystalline (1000 to 4000 µm). The finest authigenic constituents are called cryptocrystalline (less than 1µm) and aphanocrystalline with the crystal size between 1 and 4 µm.

The following describes a division within the carbonate matrix. Micrite term is used for carbonate mud that consists of 1 to 4 µm diameter crystals and forms as an inorganic precipitate or through breakdown of coarser carbonate grains. Micrite is produced within the basin of deposition and shows little or no evidence of transport (Folk, 1959). Microspar is generally 5 to 20 µm sized calcite produced by recrystallization (neomorphism) of micrite and can be as coarse as 30 µm (Folk, 1965). Microspar is restricted to recrystallization products, not primary precipitates. Calcite fabric crystal size larger than 30 to 50 µm is called a pseudospar.

## Abbreviations

The list of common thin section abbreviations in provided in the table below.

| NAME | ABBREVIATION | NAME | ABBREVIATION |
|---|---|---|---|
| Anhydrite | Anh | Intragranular Porosity | Intr. |
| Barite | Ba | Kaolinite | Kao |
| Biotite | Bio | K-Feldspar | K-Fld |
| Bioclasts (indistinct) | Biocl | Laminae | Lam |
| Burrows/Bioturbation | Bur | Metamorphic Rock Frag. | MRF |
| Bioturbation | Bt | Muscovite | Musc |
| Calcite | Cal | Matrix | Mtx |
| Carbonaceous | Carb | Micro-vuggy pore | mV |
| Chert | Cht | Organic material | OM |
| Chlorite | Chl | Phosphate | Phos |
| Concavo-convex | CC | Plutonic Rock Fragments | PRF |
| Dolomite | Dol | Polycrystalline quartz | PQ |
| Detrital Calcite | dC | Pseudo-matrix | P-mtx |
| Detrital Dolomite | dD | Pyrite | Py |
| Feldspar (plagioclase) | Fld | Quartz | Qtz |
| Ferroan Dolomite | Fe-Dol | Quartz Cement | Qc |
| Ferroan Calcite | Fe-Cal | Quartz overgrowths | Ov |
| Glauconite | Glauc | Saddle dolomite | SDol |
| Grain dissolution pore | GD | Sedimentary Rock Frag. | SRF |
| Heavy minerals | HM | Secondary porosity | SP |
| Hematite | Hem | Sutured grain contact | S |
| Illite | Ill | Volcanic Rock Fragments | VRF |
| Intergranular Porosity | IP | | |
| Intercrystalline Porosity | lxl | | |

## RESULTS

In this chapter of the report, the seven samples that were recovered from the B.A. Texaco Arrowhead B-76 300/B-76-6030-12245/0 location will be described separately. The images that show specific features of each sample will follow the tabulated sample description. Stratigraphic top of the thin section samples have been marked with an arrow placed in the upper right portion of the thin section.

## Stratigraphic Unit: Nahanni Formation

### Sample T21/S21, 8923.50ft/2719.88m

| | | | |
|---|---|---|---|
| **Well Name** | B.A. Texaco Arrowhead B-76 | **Location** | 300/B-76-6030-12245/0 |
| **Sample Type** | Thin section/SEM grain mount from a core sample | **Depth (m)** | 8923.50ft/2719.88m |
| **Stratigraphic Unit** | Nahanni Formation | **Reservoir Quality** | Poor |
| **Classification** | Dolostone | **Stain type** | ½ Dual carbonate stain |

**MINERALOGY**

| Thin Section Point counting (%) | Total bulk mineralogy | | | | | |
|---|---|---|---|---|---|---|
| | Calcite | Dolomite | Quartz | Pyrite | Clays & organics | Pyrobitumen |
| | 2 | 96 | TR | TR | 1 | 1 |
| | Framework, Matrix, Cement, and Replacement | | | | | |
| | Carbonate clasts | Bioclasts | Detrital grains | Matrix | Pore filling cement | Replacement |
| | - | 2 | TR | 1 | 3 | 94 |

**ADDITIONAL FEATURES and OTHER COMMENTS**

| | |
|---|---|
| **Depositional** | At the time of deposition, the sample was most likely lime-wackestone that has been eventually dolomitized. Formation of low amplitude stylolites typically occurs during burial diagenesis (chemical compaction). Selective dissolution and/or calcitization of dolomite (dedolomitization) occurs as patches of calcite spar cement, which could precipitate during the burial diagenesis. |
| **Textures** | Dolomite fabrics were classified as planar and nonplanar (Sibley & Gregg, 1987) based on the nature of crystal boundaries. Sibley and Gregg (1987) also divide replacement fabrics by crystal size distribution into unimodal and polymodal, and by degree of preservation of precursor fabric into mimic (fabric-preserving) and nonmimic (fabric destroying ) varieties. This sample shows nonplanar fabrics, with overall unimodal crystal size. Due to the dolomitization, the precursor rock texture was overall destroyed (nonmimic), and only in a few spots there are still visible remnants of bioclast fragments, which are totally dolomitized. |
| **Framework (Carbonate clasts, Bioclasts)** | Petrographic Summary Table 1 shows detailed mineralogy of the sample. This sample contains 92% of dolomite. Other minerals include minor calcite (2%), pyrobitumen (1%), clays and organics (1%), plus trace pyrite and quartz. clays and organics (3%), pyrite (2%), dolomite |

| | |
|---|---|
| | (1%), plus trace quartz. There are no carbonate clasts, and only minor (2%) amounts of totally dolomitized bioclasts were observed. Based on the shape, the bioclasts could possibly be thin tabular stromatoporoid fragments (Amphipora? Or Idiostroma?). |
| **Detrital Grains & Other Non-Carbonate Grains** | There are no detrital grains in this sample. Trace amounts of microcrystalline quartz cement is spotted filling intercrystalline pores. |
| **Matrix** | Minor amounts of clays and organic material that is incorporated into low amplitude stylolites has been classified as matrix of this sample. |
| **Pore Filling Cements** | The pore filling cements occur in minor amounts and include calcite spar (2%), Pyrobitumen (1%), plus trace pyrite and quartz. |
| **Replacement Minerals** | Nonplanar very coarse crystalline dolomite is the main replacement mineral. Trace amount of pyrite appears to replace organic matter within stylolites. |
| **Porosity** | There is only a trace amount of intercrystalline pores observed in this sample. |

Annotated microphotographs of the thin section and SEM samples with descriptions are provided below.

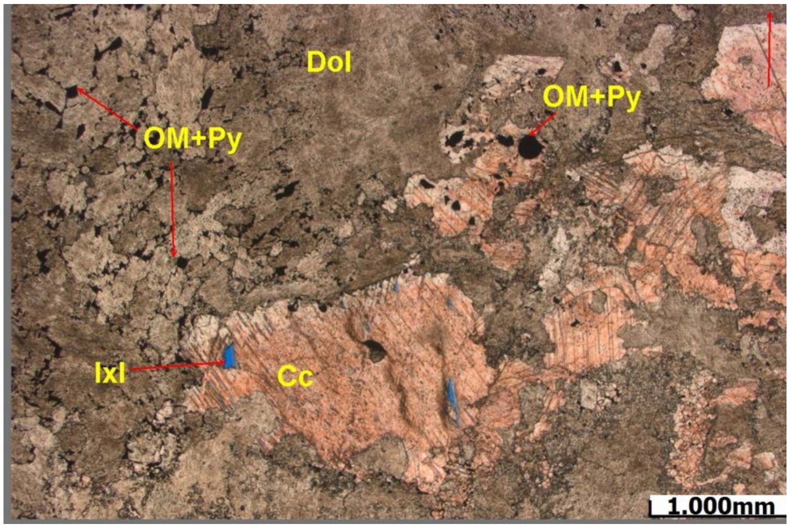


**Figure 1.1. Sample T21, 8923.50ft/2719.88m**. Low magnification overview was taken from the portion of the thin section sample that was stained for carbonates. The replacement dolomite (Dol) appears light brown, while calcite cement (Cc) is pink. Patchy dissolution and/or calcitization of dolomite (dedolomitization) occurs as calcite spar cement. Organic matter (most likely pyrobitumen) plugs intercrystalline pores (Ixl). Dolomite shows nonplanar fabrics, with overall unimodal crystal size. Some of the dolomite crystals shows sweeping extinctiin that is characteristic for saddle or baroque dolomite. **x25ppl**

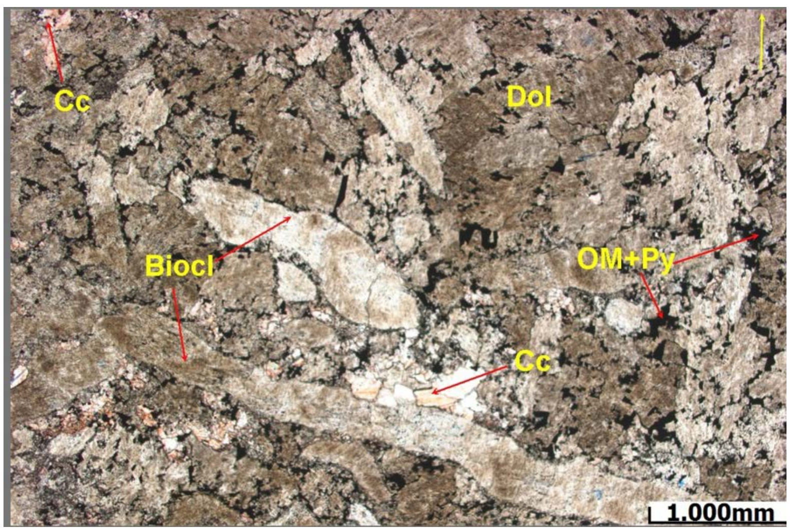


**Figure 1.2. Sample T21, 8923.50ft/2719.88m**. Alternate low magnification image shows scattered dolomitized bioclast fragments (Biocl). Based on the shape and size of these bioclasts, they were tentatively identified as Amphipora or Idiostroma. Organic matter locally encrusted with micropyrite plugs intercrystalline pores (OM+Py). Cc: calcite cement. **x25ppl**

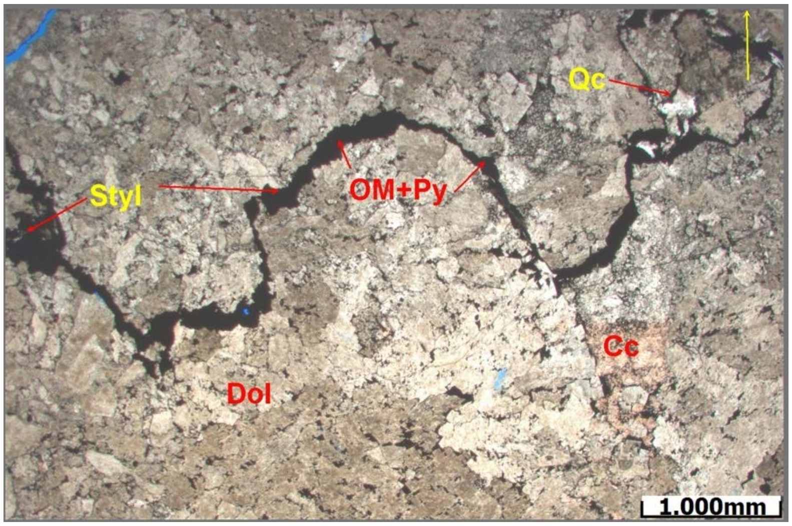


**Figure 1.3. Sample T21, 8923.50ft/2719.88m**. Another low magnification image of the sample focuses on the presence of low amplitude stylolites (Styl) that are observed in this sample. Black color of the stylolite indicates presence of organic rich clays and pyrite (OM+Py). Rare spots of quartz cement (QC) fills intercrystalline pores. Calcite spar (Cc) replaces dolomite (dedolomitization). The sample is a very coarse crystalline dolostone (Dol). There is no visible porosity in this sample. **x25ppl**

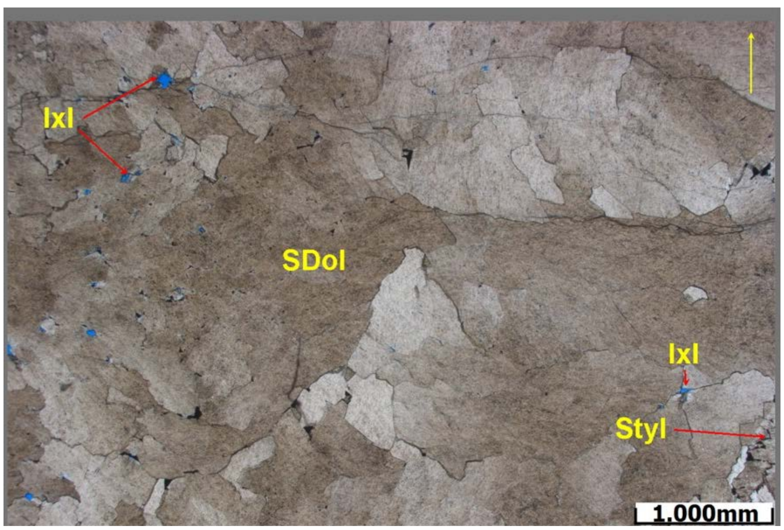


**Figure 1.4. Sample T21, 8923.50ft/2719.88m**. The next two images shows the nonplanar, closely packed 'saddle' dolomite crystals (SDol) with curved crystal faces, cloudy appearance (fluid and/or mineral inclusions) and undulose extinction in cross polarized light (see Figure 1.5). The intercrystalline pores are rare and poorly interconnected (Ixl). Tiny vertical stylolite (Styl) is observed at the bottom right portion of the image. **x25ppl**

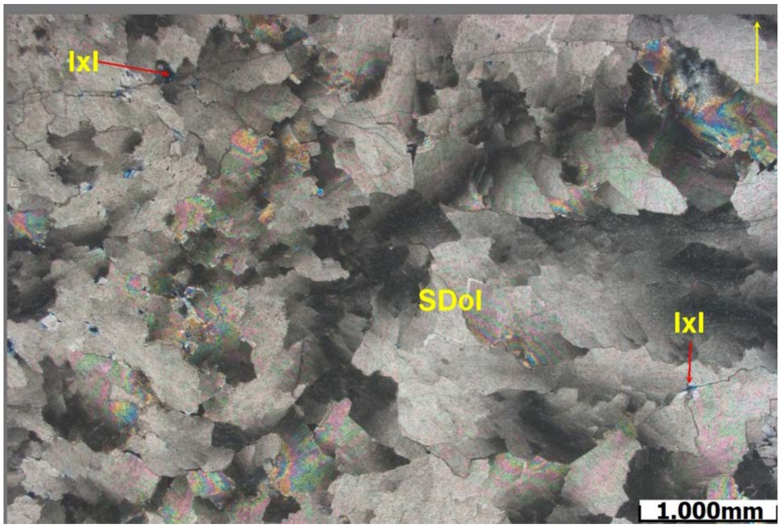


**Figure 1.5. Sample S21, 8923.50ft/2719.88m**. The image was taken from the same portion of the thin section sample, but under cross polarized light condition to accentuate sweeping extinction of 'saddle dolomite' crystals. Ixl: intercrystalline pores. **x25ppl**

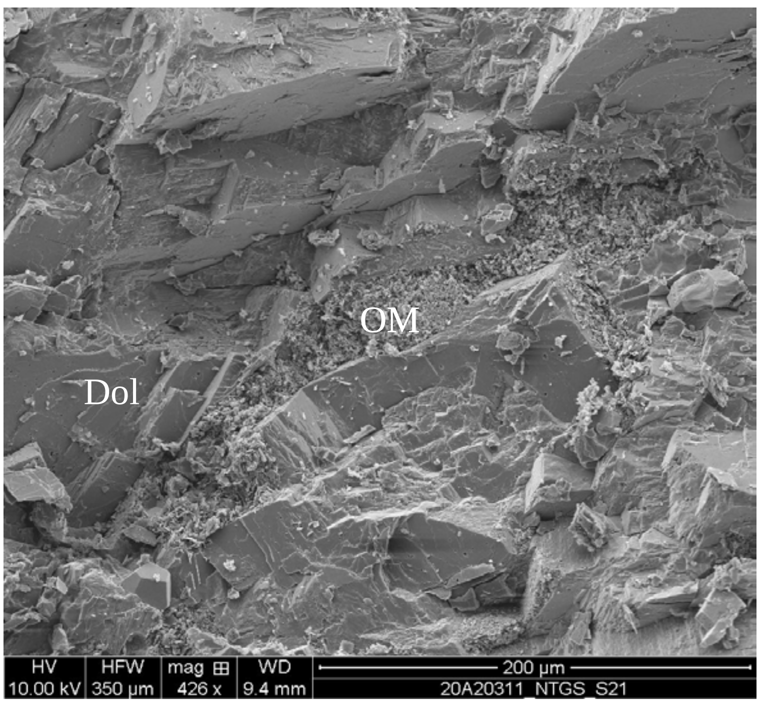


**Figure 1.6. Sample S21, 8923.50ft/2719.88m.** Low magnification scanning electron microscope (SEM) image highlighting a localized concentration of fine organics (OM), likely representing a styloloite, within blocky dolomite (Dol). **x426**

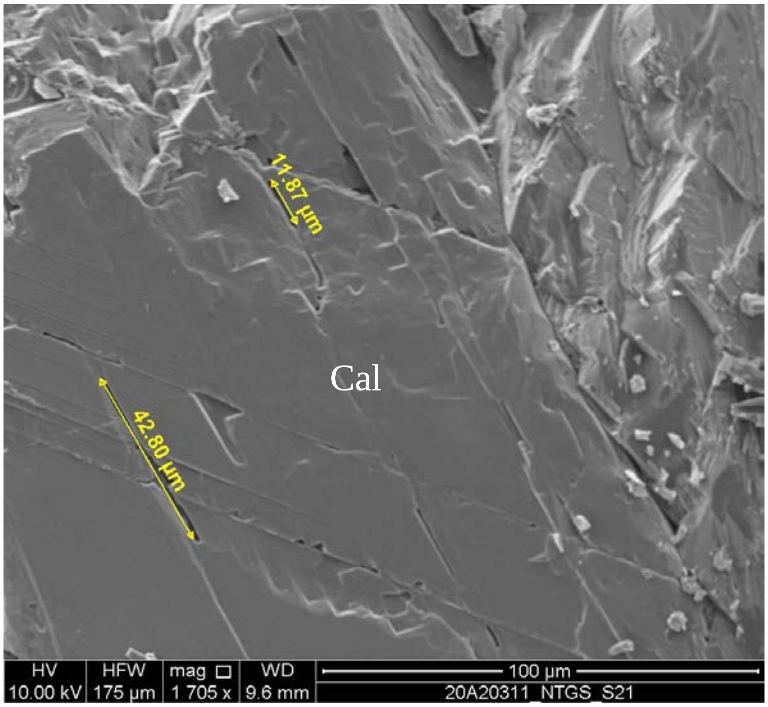


**Figure 1.7. Sample S21, 8923.50ft/2719.88m.** Moderate magnification scanning electron microscope (SEM) image of elongate intracrystalline pores associated with sparry calcite cement (Cal). **x1705**

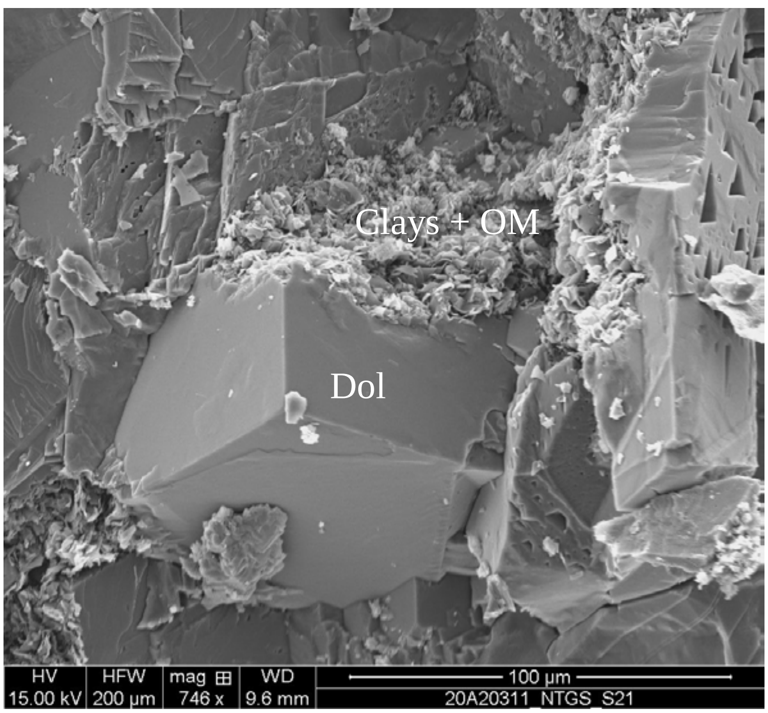


**Figure 1.8. Sample S21, 8923.50ft/2719.88m.** Low magnification scanning electron microscope (SEM) image showing interstitial clays and fine organic material (Clays + OM). Dol: dolomite. **x746**

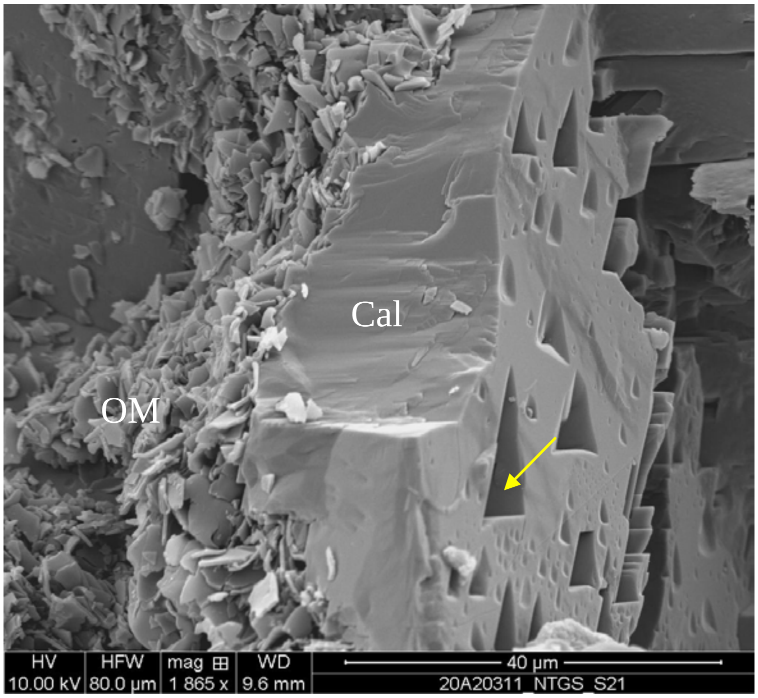


**Figure 1.9. Sample S21, 8923.50ft/2719.88m.** Moderate magnification scanning electron microscope (SEM) image showing details of the organic material (OM) shown in Figure 1.8. Calcite (Cal) shows interesting intracrystalline pores (yellow arrow) that may aid in increasing reservoir volume, but are likely ineffective. **x1865**

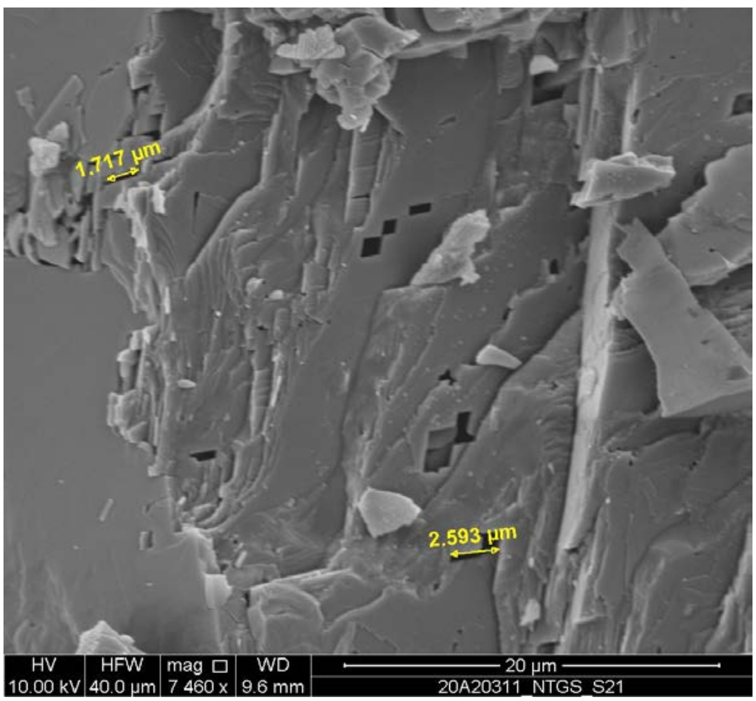


**Figure 1.10. Sample S21, 8923.50ft/2719.88m.** High magnification scanning electron microscope (SEM) image showing scattered intra- and intercrytalline pores associated with dolomite. **x7460**

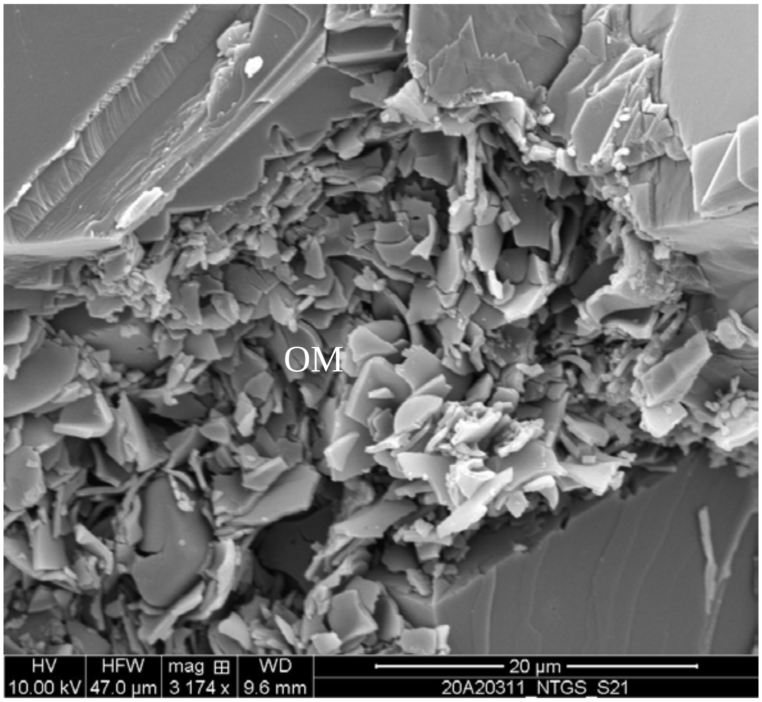


**Figure 1.11. Sample S21, 8923.50ft/2719.88m.** High magnification scanning electron microscope (SEM) image of platy organic debris (OM). **x3174**

## Sample T20/X39/S20, 8927.00ft/2720.95m

| | | | |
|---|---|---|---|
| **Well Name** | B.A. Texaco Arrowhead B-76 | **Location** | 300/B-76-6030-12245/0 |
| **Sample Type** | Thin section/SEM grain mount from a core sample | **Depth (m)** | 8927.00ft/2720.95m |
| **Stratigraphic Unit** | Nahanni Formation | **Reservoir Quality** | Poor |
| **Classification** | Limestone (Grainstone) | **Stain type** | ½ Dual carbonate stain |

**MINERALOGY**

| | Total Bulk mineralogy | | | | | |
|---|---|---|---|---|---|---|
| Thin Section Point counting (%) | Calcite | Dolomite | Quartz | Pyrite | Clays & organics | Pyrobitumen |
| | 97 | | - | TR | 2 | 1 |
| | Framework, Matrix, Cement, and Replacement | | | | | |
| | Carbonate clasts | Bioclasts | Detrital grains | Matrix | Pore filling cement | Replacement |
| | - | 95 | - | 4 | 1 | TR |

**ADDITIONAL FEATURES and OTHER COMMENTS**

| | |
|---|---|
| **Depositional** | The sample is massive with no distinct sedimentary features. |
| **Textures** | Based on the mineralogy, abundance of bioclasts, and low amounts of micrite, the sample was classified as lime-grainstone. For the matrix, the crystal texture has been determined as anhedral, while crystalline cement, which is only observed as syntaxial overgrowths on crinoidal debris show euhedral to subhedral crystal texture. The fabric of the grainstone locally shows sutured contact between individual clasts. |
| **Framework (Carbonate clasts, Bioclasts)** | The framework of this grainstone comprises crinoids (45%), with lesser corals (30%), and stromatoporoid (20%). |
| **Detrital Grains & Other Non-Carbonate Grains** | There are no detrital grains in this sample. |
| **Matrix** | Overall minor amounts of matrix (4%) consist of calcite micrite (2%) and clays and organics (2%) that define sutured contacts between allochems. |
| **Pore Filling Cements** | Minor amounts of pyrobitumen (1%) locally obstructs primary interparticle pores. |
| **Replacement Minerals** | Trace amounts of pyrite replaces micrite within the matrix and micritized framework grains. |
| **Porosity** | There is no visible porosity in this sample. |

The annotated microphotographs of the thin section and SEM samples with descriptions are provided below.

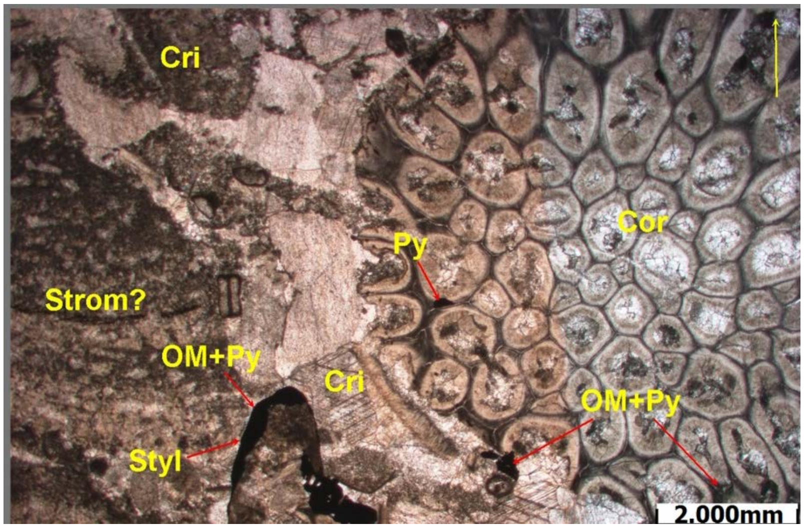


**Figure 2.1. Sample T20, 8927.00ft/2720.95m**. Low magnification overview of the sample shows a transverse section through the colonial tabulate coral (Cor). The close packing of polygonal corallites and lack of internal septal partitions, and the brownish calcite of corallite walls are still visible in this image. Tiny pyrite framboids locally replaces micrite within corallite walls. Possible tabular stromatoporoid (Strom?) and crinoid debris (Cri) are the other bioclasts in this sample. Stylolitized laminae (Styl) is defined by the accumulation of organic matter and pyrite (OM+Py). **x12.5ppl**

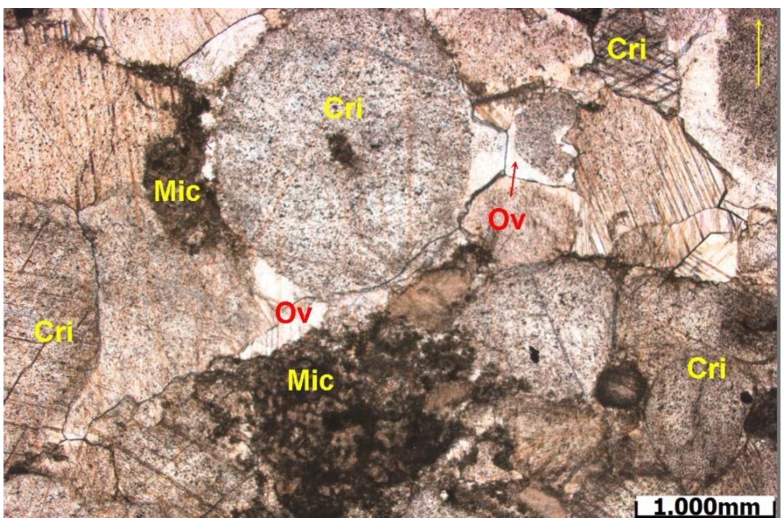


**Figure 2.2. Sample T20, 8927.00ft/2720.95m**. Another low magnification image of the sample shows tightly packed Crinoid plates (Cri) that are cemented by their overgrowths (Ov). Small amounts of micrite (Mic) fills interparticle porosity. Some of the crinoids plates are possibly micritized as well (bottom-center). **x25ppl**

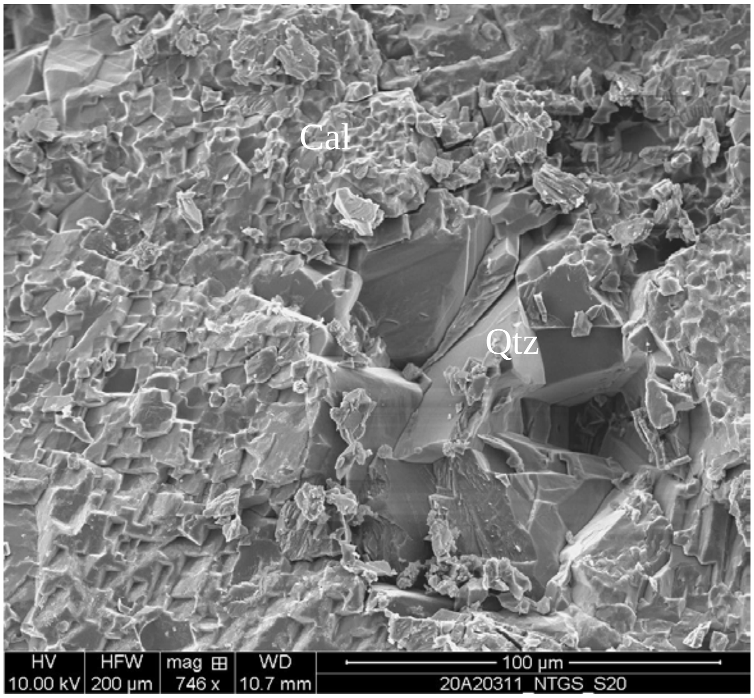


**Figure 2.3. Sample S20, 8927.00ft/2720.95m.** Low magnification scanning electron microscope (SEM) image showing secondary quartz (Qtz) within a calcite micrite matrix (Cal). Porosity is poor within this view. **x746**

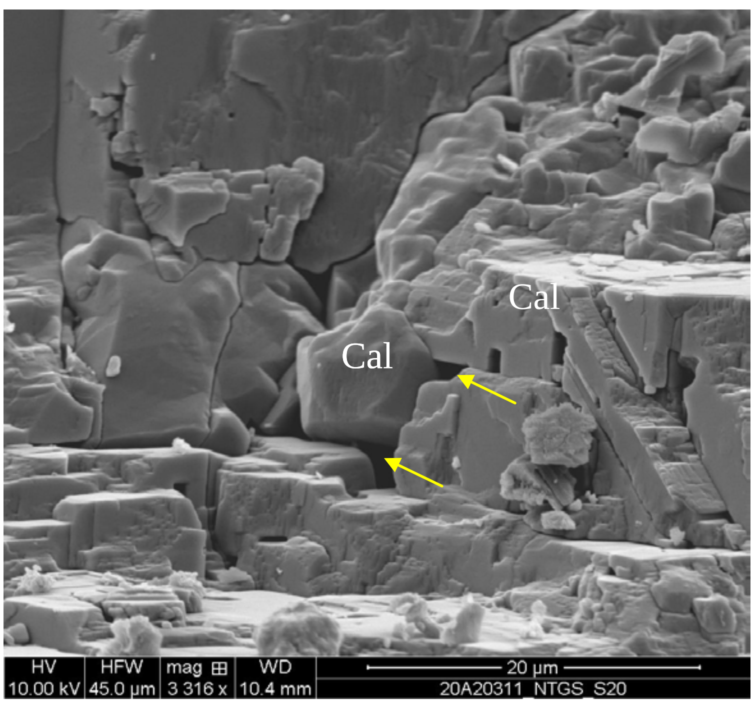


**Figure 2.4. Sample S20, 8927.00ft/2720.95m.** Moderate magnification scanning electron microscope (SEM) image showing localized micropores (yellow arrows). Cal: calcite. **x3316**

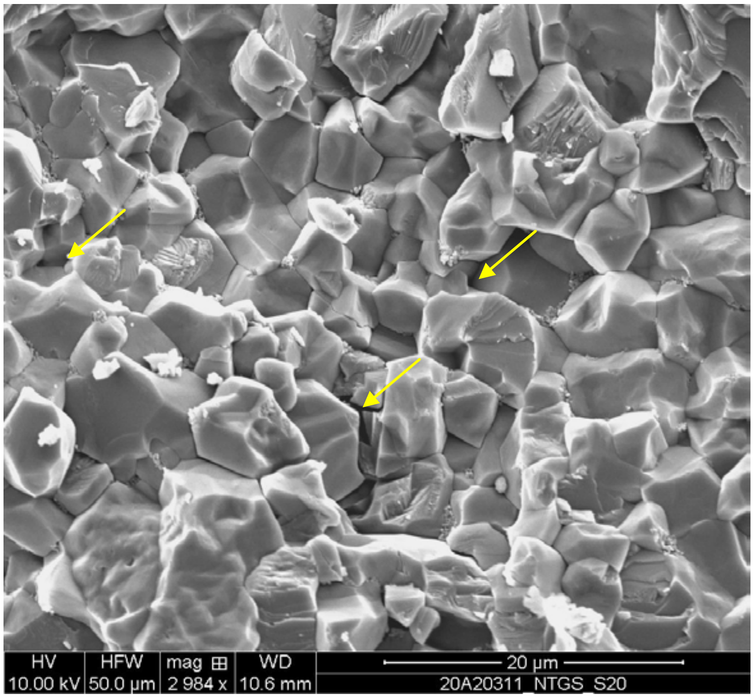


**Figure 2.5. Sample S20, 8927.00ft/2720.95m.** Moderate magnification scanning electron microscope (SEM) image highlighting microporosity (yellow arrows) associated with the micritic matrix. **x2984**

## Sample T19/ X38/ S19, 8946.30ft/2726.83m

| | | | |
|---|---|---|---|
| **Well Name** | B.A. Texaco Arrowhead B-76 | **Location** | 300/B-76-6030-12245/0 |
| **Sample Type** | Thin section/SEM grain mount from a core sample | **Depth (m)** | 8946.30ft/2726.83m |
| **Stratigraphic Unit** | Nahanni Formation | **Reservoir Quality** | Poor |
| **Classification** | Limestone (Wackestone) | **Stain type** | ½ Dual carbonate stain |

**MINERALOGY**

| | Total Bulk mineralogy | | | | | |
|---|---|---|---|---|---|---|
| **Thin Section Point counting (%)** | **Calcite** | **Dolomite** | **Quartz** | **Pyrite** | **Phosphate** | **Clays & organics** |
| | 99 | - | TR | 1 | TR | TR |
| | **Framework, Matrix, Cement, and Replacement** | | | | | |
| | **Carbonate clasts** | **Bioclasts** | **Detrital grains** | **Matrix** | **Pore filling cement** | **Replacement** |
| | - | 50 | TR | 39 | 10 | 1 |

**ADDITIONAL FEATURES and OTHER COMMENTS**

| | |
|---|---|
| **Depositional** | The sample is massive to faintly laminated. Relatively large size crack or sub-vertical fracture that is totally healed with calcite spar is also observed (see Figure 3.1). |
| **Textures** | The sample is a bioclastic wackestone. The crystal texture of the matrix is anhedral, while cement shows euhedral crystal texture. |
| **Framework (Carbonate clasts, Bioclasts)** | The framework of this grainstone is dominated by crinoids (25%), with lesser mollusks (10%) and ostracodes (10%), plus minor brachiopod (5%). Note that the majority of the bioclasts are highly fragmented, impossible to identify, and they were accounted as a part of the matrix. |
| **Detrital Grains & Other Non-Carbonate Grains** | Some of the ostracode carapaces are composed appears to be composed of phosphate. |
| **Matrix** | Abundant matrix (39%) is divided into calcite-micrite (37%), microspar (2%), plus trace amounts of clays and organic matter. As it was mentioned above, the fragmented bioclast fragments are also part of the matrix. |
| **Pore Filling Cements** | Calcite spar (10%) is the pore filling cement. |
| **Replacement Minerals** | Minor amounts of pyrite (1%) replaces micrite within the matrix and micritized framework grains, while microcrystalline quartz locally replaces ostracode and mollusks shell fragments (see Figures 3.1 and 3.3). |
| **Porosity** | There is no visible porosity in this sample |

Annotated microphotographs of the thin section and SEM samples with descriptions are provided below.

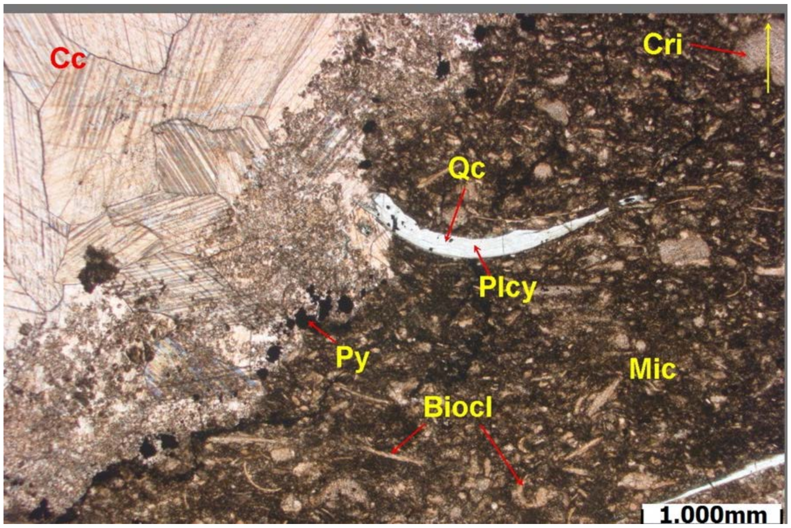


**Figure 3.1. Sample T19, 8946.30ft/2726.83m.** Low magnification overview of the bioclastic wackestone. Rare crinoid plates (Cri) and quartz replaced (Qc) pelecypod shell fragments are surrounded by abundant matrix. The matrix consists of calcite micrite (Mic) and fragmented indistinct bioclasts (Biocl). On the left hand side of the image there is sub-vertical cracks or fracture, which is total healed with calcite spar (Cc).. Note pyrite (Py) framboids accumulation along the fracture. **x25ppl**

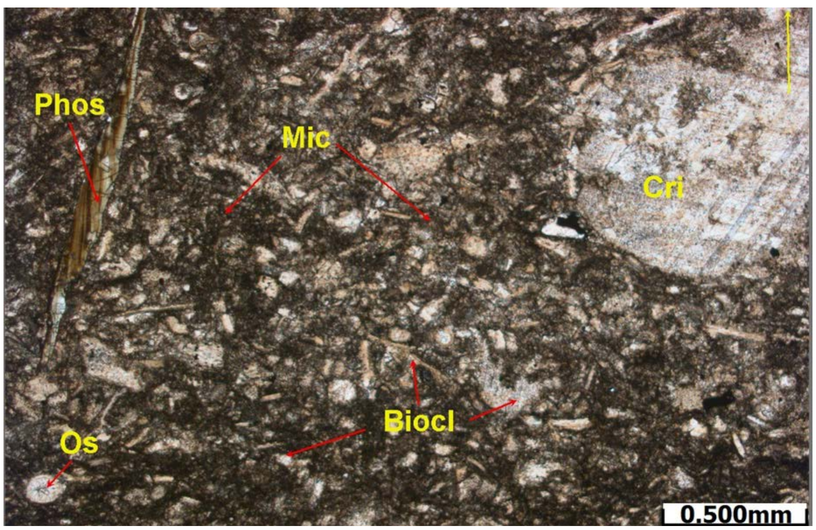


**Figure 3.2. Sample T19, 8946.30ft/2726.83m.** Moderate magnification image of the wackestone shows large sized crinoid plates (Cri) and phosphatic shell fragments (Phos) floating in the bioclastic-micrite matrix (Biocl; Mic). The majority of the bioclasts that are a part of the matrix are highly fragmented and impossible to identify. Only occasionally small ostracode fragments (Os) with the interior filled by calcite spar were observed. **x50ppl**

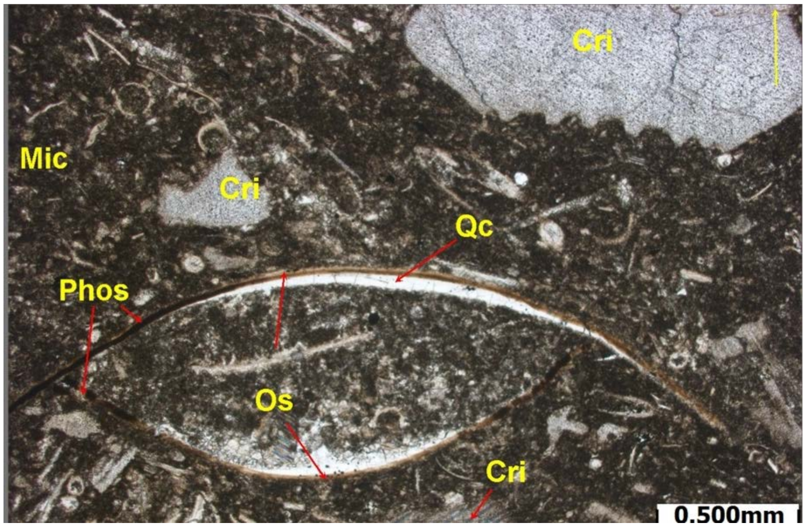


**Figure 3.3. Sample T19, 8946.30ft/2726.83m.** Another moderate image of the sample shows a longitudinal section of crinoid steam (top-right) and large sized phosphatic (Phos) ostracode (Os) carapaces, which are partly replaced by authigenic quartz (Qc). Note that the ostracode valve at the top portion of the image overlaps the bottom valve, which is very common for ostracodes. Interior of the ostracode has been leached and filled with micrite (Mic). **x50ppl**

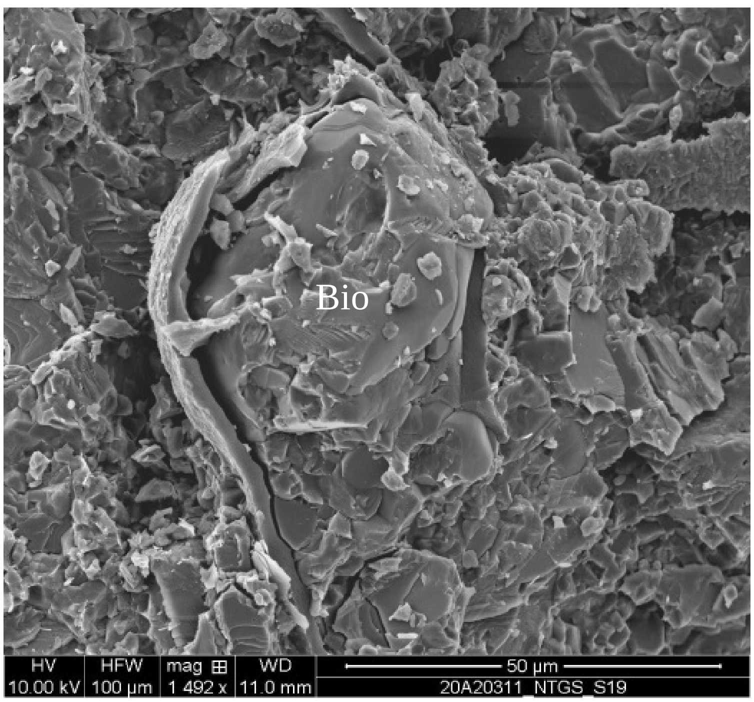


**Figure 3.4. Sample S19, 8946.30ft/2726.83m.** Moderate magnification scanning electron microscope (SEM) image of a bioclast (Bio) showing that the internal cavity has been infilled with carbonate cement. **x1492**

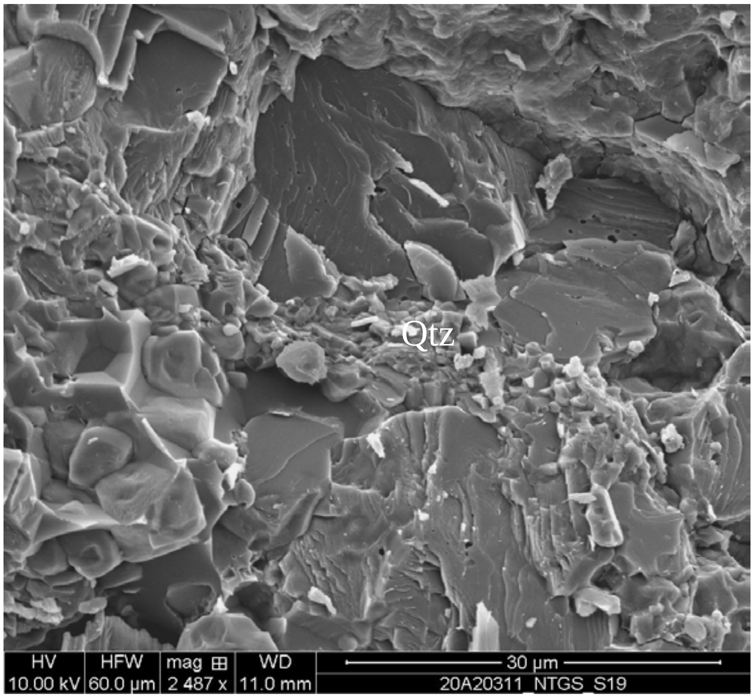


**Figure 3.5. Sample S19, 8946.30ft/2726.83m.** High magnification scanning electron microscope (SEM) image showing localized quartz microcrytallites (Qtz). This is consistent with thin section observation which shows localized replacement of bioclasts by secondary quartz cement. **x2487**

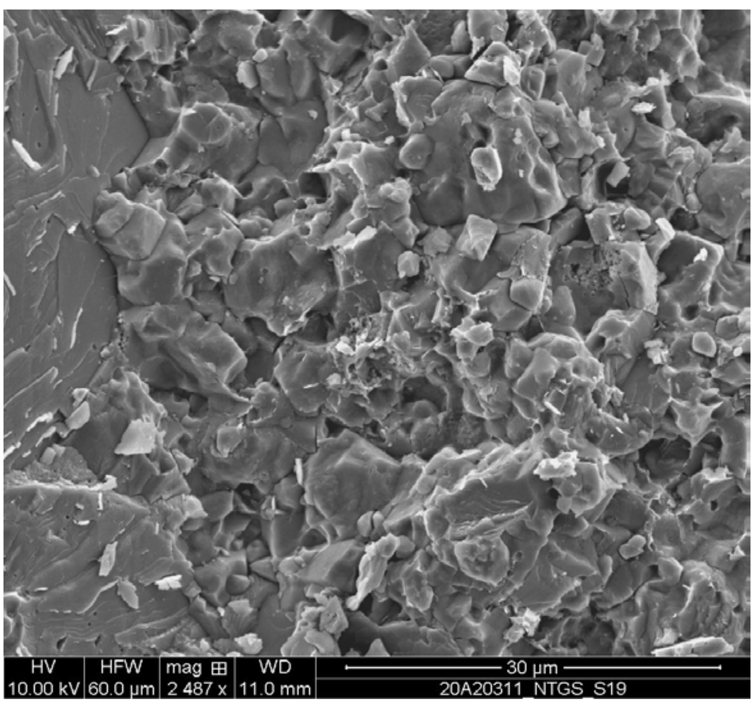


**Figure 3.6. Sample S19, 8946.30ft/2726.83m.** Moderate magnification scanning electron microscope (SEM) image of the microporous micritic matrix. **x2487**

## Sample T18/ X37/ S18/ P11, 8963.25ft/2732.00m

| | | | |
|---|---|---|---|
| **Well Name** | B.A. Texaco Arrowhead B-76 | **Location** | 300/B-76-6030-12245/0 |
| **Sample Type** | Thin section/SEM grain mount from a core sample | **Depth (m)** | 8963.25ft/2732.00m |
| **Stratigraphic Unit** | Nahanni Formation | **Reservoir Quality** | Poor |
| **Classification** | Dolostone | **Stain type** | ½ Dual carbonate stain |

**MINERALOGY**

| | Total bulk mineralogy | | | | | |
|---|---|---|---|---|---|---|
| Thin Section Point counting (%) | Calcite | Dolomite | Quartz | Pyrite | Pyrobitumen | |
| | TR | 97 | TR | 2 | 1 | |
| | Framework, Matrix, Cement, and Replacement | | | | | |
| | Carbonate clasts | Bioclasts | Detrital grains | Matrix | Pore filling cement | Replacement |
| | - | TR | - | - | 3 | 97 |

**ADDITIONAL FEATURES and OTHER COMMENTS**

| | |
|---|---|
| **Depositional** | The sample is almost totally dolomitized; therefore it is impossible to determine original structure of the precursor rock. |
| **Textures** | The dolomite shows nonplanar fabrics, with overall unimodal crystal size. Due to the dolomitization, the precursor rock texture was totally destroyed (nonmimic). |
| **Framework (Carbonate clasts, Bioclasts)** | Petrographic Summary Table 1 shows detailed mineralogy of the sample. This sample contains 97% of dolomite. Other minerals include minor pyrite (2%) and pyrobitumen (1%), plus trace calcite and quartz. There are no carbonate clasts, and only trace amount of indistinct un-dolomitized bioclast fragments are observed. |
| **Detrital Grains & Other Non-Carbonate Grains** | There are no detrital grains in this sample. |
| **Matrix** | There is no matrix in this sample. |
| **Pore Filling Cements** | The pore filling cements occur in minor amounts and include pyrite (2%), pyrobitumen (1%), plus trace quartz. |
| **Replacement Minerals** | Nonplanar very coarse crystalline dolomite is the replacement mineral. The majority of the dolomite is a saddle or baroque type and shows sweeping extinction. |
| **Porosity** | There is only a trace amount of intercrystalline and micro-vuggy pores observed in this sample. The RCA reports porosity of 1% and gas permeability of 5.66mD. Note that high gas permeability is due to fractures in the core plug. |

Annotated microphotographs of the thin section and SEM samples with descriptions can be found below.

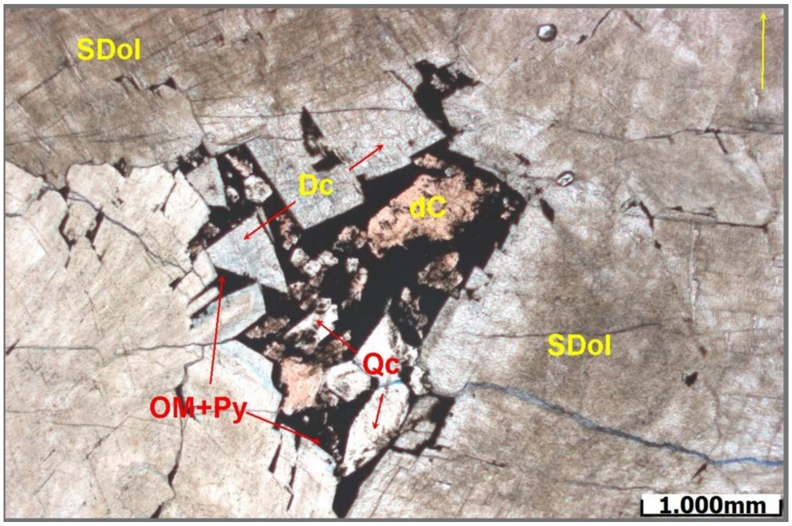


**Fig 4.1. Sample T18, 8963.25ft/2732.00m.** Low magnification overview image highlights a micro-vuggy pore (middle) that has been plugged by multiple generation of cements such as euhedral dolomite rhombs (Dc), authigenic quartz (Qc) and pyrobitumen that appears to contain finely disseminated micropyrite (OM+Py). The replacement dolomite is a saddle dolomite (SDol). Note a remnant of calcitic (un-dolomitized) bioclast fragment (dC). **x25ppl**

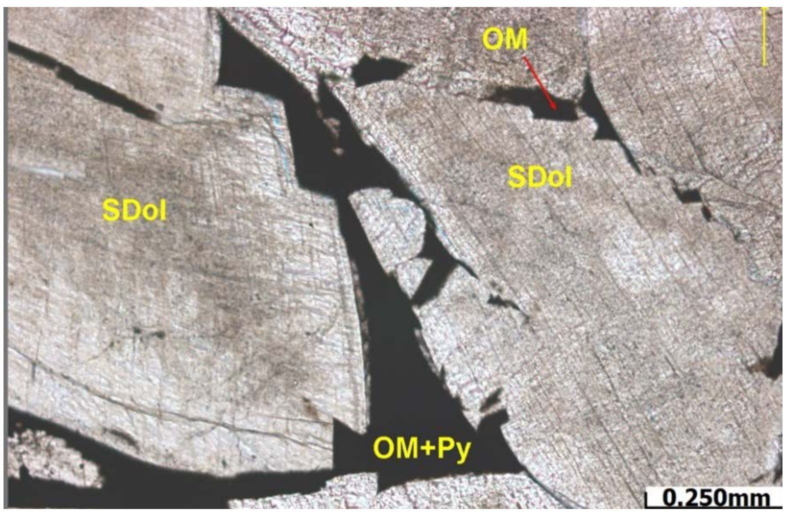


**Figure 4.2. Sample T18, 8963.25ft/2732.00m.** High magnification image shows the intercrystalline pores totally filled with pyrobitumen, which is locally intermixed with micropyrite (OM; OM+Py). The replacement dolomite in this image is a saddle dolomite (SDol) that shows curved crystal faces and undulose extinction. **x100ppl**

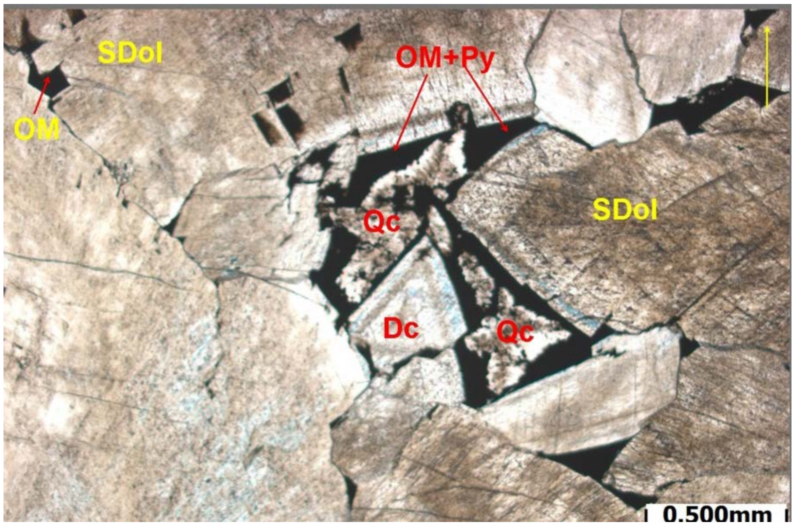


**Figure 4.3. Sample T18, 8963.25ft/2732.00m.** Moderate magnification image shows a few generations of cements that filled intercrystalline and/or micro-vuggy pores. In the middle of this image a dissolution enlarged intercrystalline pores (micro-vugs) have been plugged with quartz cement (Qc), followed by slightly ferroan (rim) euhedral dolomite (Dc) and pyrobitumen (OM+Py). The other intercrystalline pores have been plugged by pyrobitumen (OM). Saddle dolomite (SDol) is the replacement mineral observed in this very coarse crystalline dolostone sample. **x50ppl**

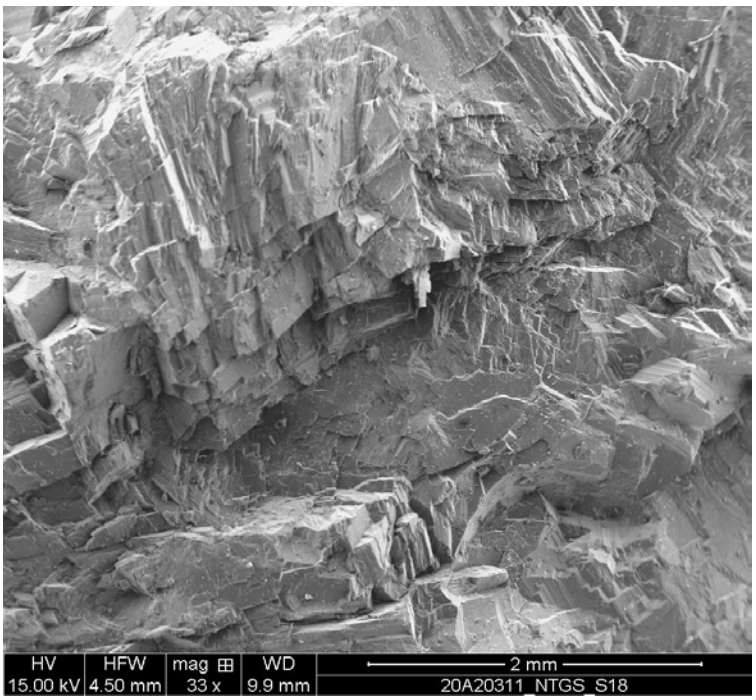


**Figure 4.4. Sample S18, 8963.25ft/2732.00m.** Low magnification scanning electron microscope (SEM) image highlighting coarse crystalline dolomite. Visible porosity within this view is lacking due to the interlocking crystal fabric. **x33**

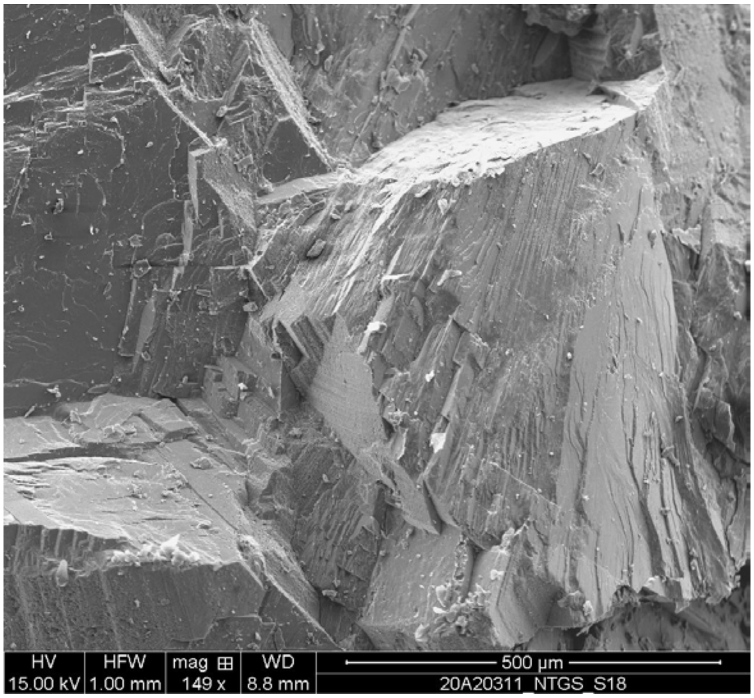


**Figure 4.5. Sample S18, 8963.25ft/2732.00m.** Low magnification scanning electron microscope (SEM) image showing dolomite with curved crystal faces and cleavage planes consistent with saddle dolomite. **x149**

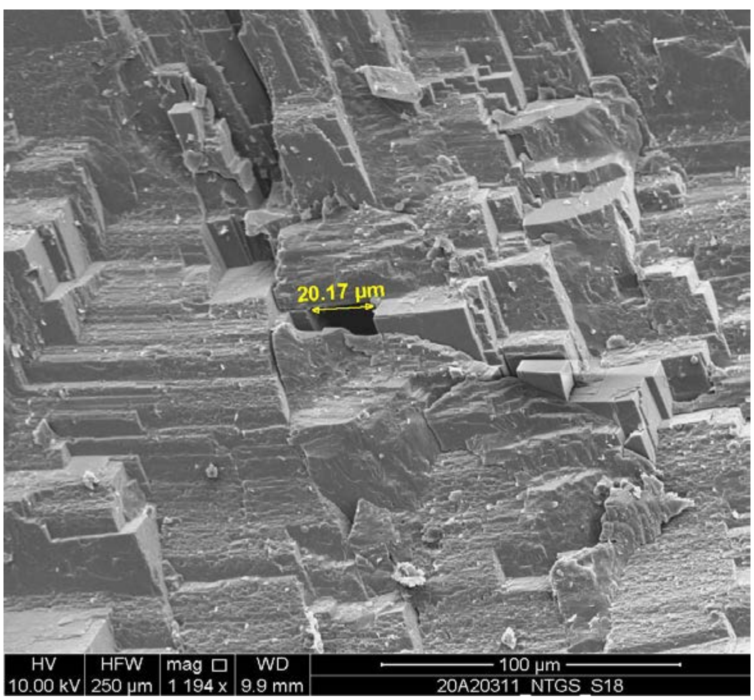


**Figure 4.6. Sample S18, 8963.25ft/2732.00m.** Moderate magnification scanning electron microscope (SEM) image of a macropore (~20μm) within blocky dolomite crystals. **x1194**

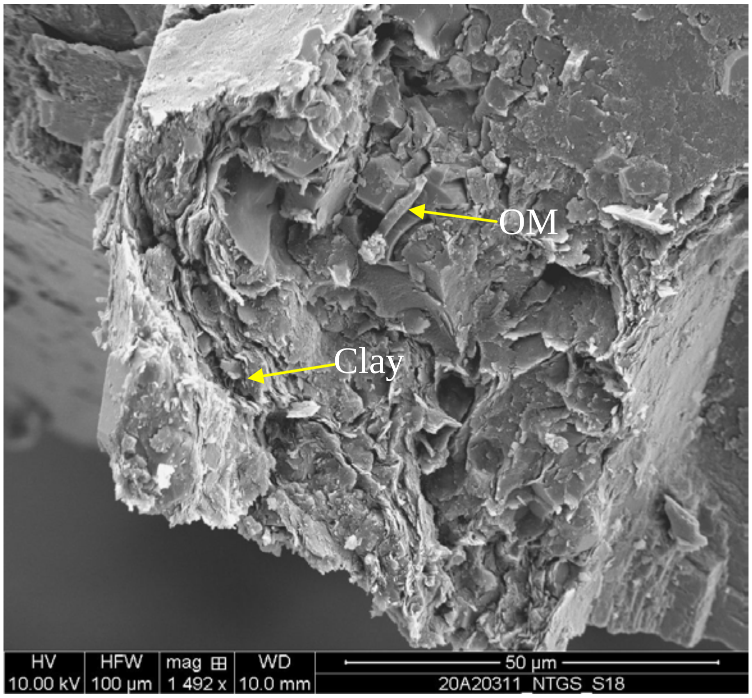


**Figure 4.7. Sample S18, 8963.25ft/2732.00m.** Moderate magnification scanning electron microscope (SEM) image showing platy clays (Clay), probable illite, plus organic matter (OM) that locally plugs pore spaces in this sample. **x1492**

## Sample T17/X36/ S17/ P10, 8988.20ft/2739.60m

| | | | |
|---|---|---|---|
| **Well Name** | B.A. Texaco Arrowhead B-76 | **Location** | 300/B-76-6030-12245/0 |
| **Sample Type** | Thin section/SEM grain mount from a core sample | **Depth (m)** | 8988.20ft/2739.60m |
| **Stratigraphic Unit** | Nahanni Formation | **Reservoir Quality** | Poor |
| **Classification** | Dolostone | **Stain type** | ½ Dual carbonate stain |

**MINERALOGY**

| | Total bulk mineralogy | | | | | |
|---|---|---|---|---|---|---|
| Thin Section Point counting (%) | Calcite | Dolomite | Quartz | Pyrite | Pyrobitumen | Clays & organics |
| | 1 | 93 | 4 | TR | 2 | TR |
| | Framework, Matrix, Cement, and Replacement | | | | | |
| | Carbonate clasts | Bioclasts | Detrital grains | Matrix | Pore filling cement | Replacement |
| | - | - | - | TR | 7 | 93 |

**ADDITIONAL FEATURES and OTHER COMMENTS**

| | |
|---|---|
| Depositional | This sample is a dolostone that does not show any remnants of the original sedimentary structure of the precursor rock. |
| Textures | The dolomite shows nonplanar fabrics, with overall unimodal crystal size. Due to the dolomitization, the precursor rock texture was totally destroyed (nonmimic). |
| Framework (Carbonate clasts, Bioclasts) | This sample contains 93% of dolomite. Other minerals include minor pyrobitumen (2%) and calcite (1%), plus trace pyrite and clays & organics. There are no framework grains (carbonate clasts or bioclasts). |
| Detrital Grains & Other Non-Carbonate Grains | There are no detrital grains in this sample. |
| Matrix | Trace amounts of matrix consists of clays and organic matter. |
| Pore Filling Cements | The pore filling cements occur in minor amounts and include, authigenic quartz (4%), pyrobitumen (2%), calcite spar (1%), plus trace pyrite. |
| Replacement Minerals | Nonplanar very coarse crystalline dolomite is the replacement mineral. The majority of the dolomite is a saddle or baroque type and shows sweeping extinction. |
| Porosity | There is only a minor amount of micro-vuggy (3%) and intercrystalline (1%) pores observed in this sample. The helium RCA porosity that was measured on a core plug is reported as 3.1%. The gas permeability of the core plug is very high (42mD) due to fractures (both induced and natural). |

Annotated microphotographs of the thin section and SEM samples with descriptions are provided in the next four pages.

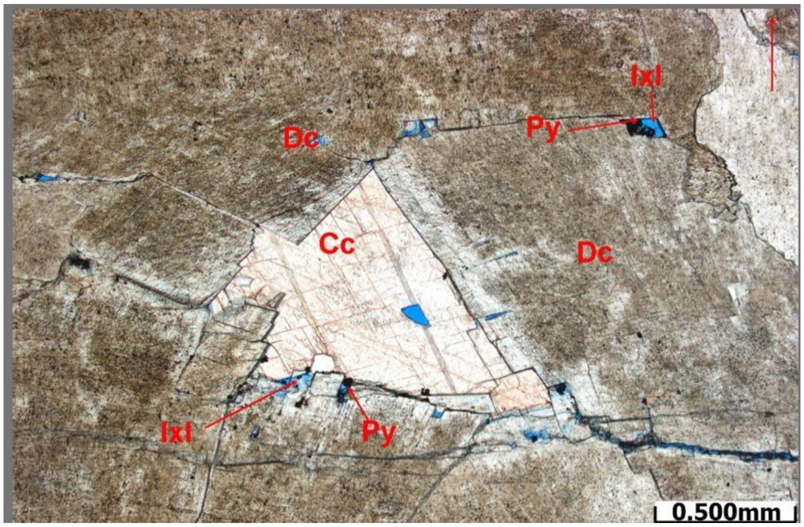


**Figure 5.1. Sample T17, 8988.20ft/2739.60m.** Moderate magnification image of the thin section shows micro-vuggy or dissolution enlarged intercrystalline pore that has been filled by calcite spar (Cc). Some of the intercrystalline pores (Ixl) are partly plugged with pyrite framboids (Py). Dc: replacement dolomite **x50ppl**

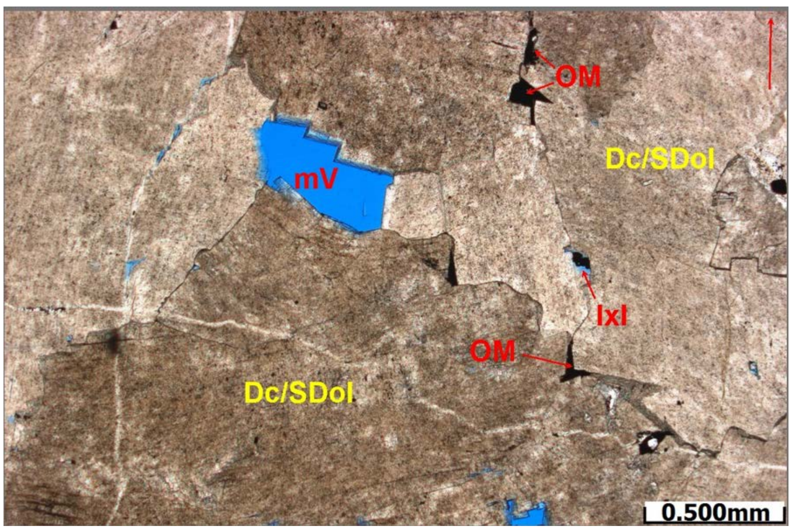


**Figure 5.2. Sample T17, 8988.20ft/2739.60m.** Another moderate magnification image shows coarse crystalline and saddle type replacing dolomite (Dc/SDol) with occasional intercrystalline (Ixl) and micro-vuggy pores (mV). Pyrobitumen (OM) locally plugs intercrystalline pores. **x50ppl**

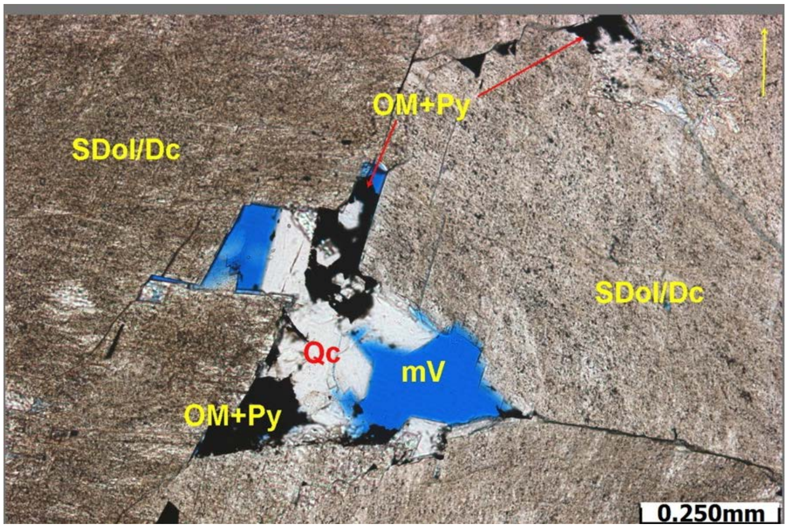


**Figure 5.3. Sample T17, 8988.20ft/2739.60m.** High magnification image shows a micro-vuggy (mV) pore that has been partly occluded by authigenic quartz cement (Qc) followed by pyrobitumen (OM+Py). Note that pyrobitumen shows micropyrite inclusions. The replacement dolomite occurs as very coarse crystalline and saddle phase of dolomite (SDol/Dc). Note that pyrobitumen locally totally fills intercrystalline pores (upper right). **x100ppl**

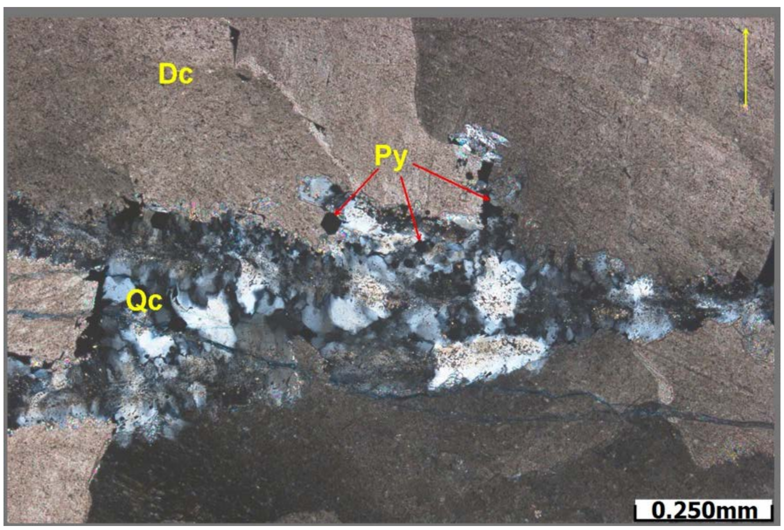


**Figure 5.4. Sample T17, 8988.20ft/2739.60m.** Another high magnification image was taken under cross polarized light condition to show megaquartz cement (Qc) that is often spotted within tiny cracks and/or fractures. Occasional pyrite framboids (Py) replace quartz cement. Dc: very coarse crystalline replacement dolomite. **x100xpl**

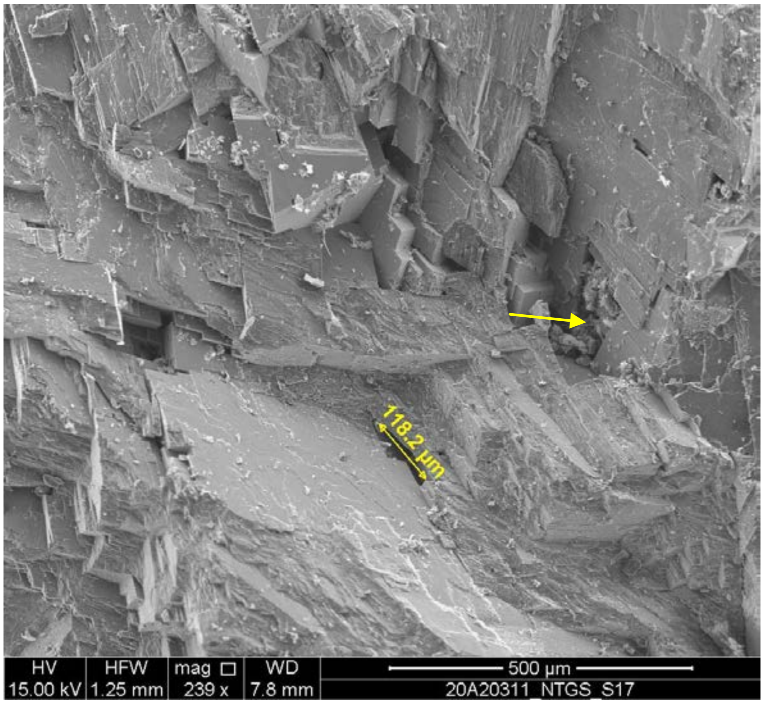


**Figure 5.5. Sample S17, 8988.20ft/2739.60m.** Low magnification scanning electron microscope (SEM) image showing an intercrystalline pore space that measures ~120µm. Clays are noted to occlude a pore space within this view (yellow arrow). **x239**

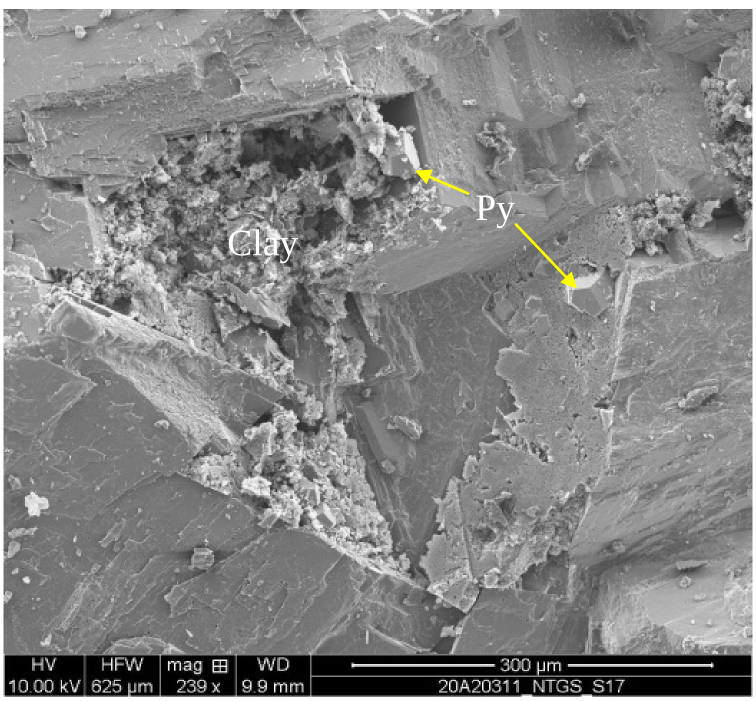


**Figure 5.6. Sample S17, 8988.20ft/2739.60m.** Alternate low magnification scanning electron microscope (SEM) image of pore occluding clays (Clay) and euhedral pyrite (Py). **x239**

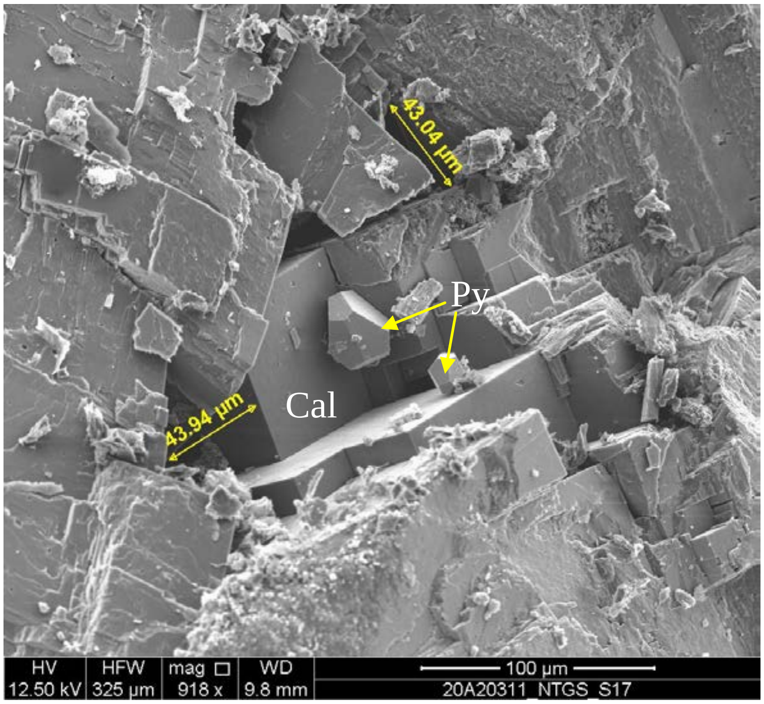


**Figure 5.7. Sample S17, 8988.20ft/2739.60m.** Scanning electron microscope (SEM) image showing a microvug that has been partly occluded by calcite (Cal) and pyrite (Py) cements; however, pore spaces measuring ~43µm have been preserved. **x918**

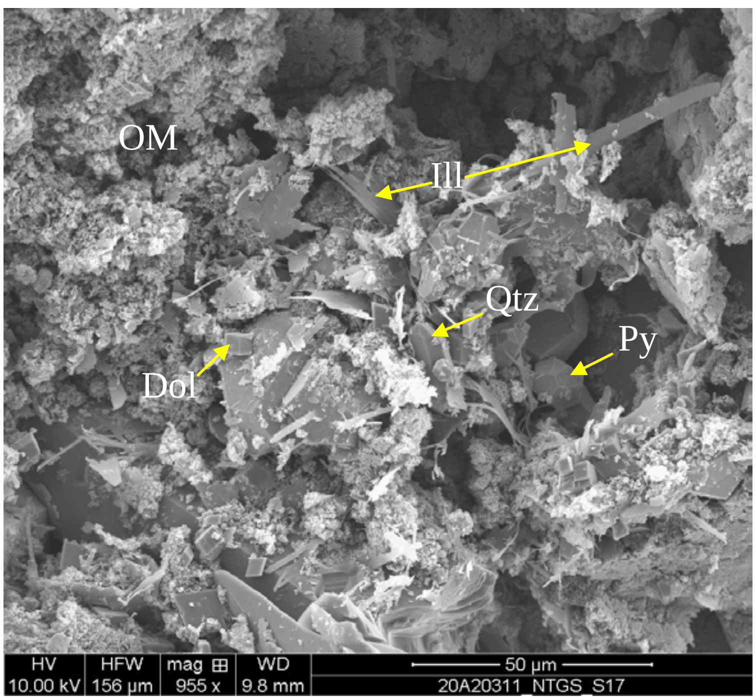


**Figure 5.8. Sample S17, 8988.20ft/2739.60m.** Scanning electron microscope (SEM) image showing an aggregate that consists of filamentous authigenic illite (Ill), fine organics (OM), in addition to euhedral dolomite (Dol), quartz (Qtz) and pyrite (Py). **x995**

## Sample T16/ S16/ P8, 9000.40ft/2743.32m

| | | | |
|---|---|---|---|
| **Well Name** | B.A. Texaco Arrowhead B-76 | **Location** | 300/B-76-6030-12245/0 |
| **Sample Type** | Thin section/SEM grain mount from a core sample | **Depth (m)** | 9000.40ft/2743.32m |
| **Stratigraphic Unit** | Nahanni Formation | **Reservoir Quality** | Poor |
| **Classification** | Limestone (Mudstone) | **Stain type** | ½ Dual carbonate stain |

**MINERALOGY**

| | Total bulk mineralogy | | | | | |
|---|---|---|---|---|---|---|
| Thin Section Point counting (%) | Calcite | Dolomite | Quartz | Pyrite | Clays & organics | |
| | 94 | 5 | - | 1 | TR | |
| | Framework, Matrix, Cement, and Replacement | | | | | |
| | Carbonate clasts | Bioclasts | Detrital grains | Matrix | Pore filling cement | Replacement |
| | - | 10 | - | 74 | 11 | 5 |

**ADDITIONAL FEATURES and OTHER COMMENTS**

| | |
|---|---|
| Depositional | At the time of deposition, the sample was most likely massive and moderately burrowed/bioturbated (mainly indistinct horizontal burrows). Development of sub-vertical fractures, which are in this sample healed with calcite spar and medium crystalline dolomite, occurred during burial diagenesis (mechanical and chemical compaction). |
| Textures | Based on the mineralogy and proportion between framework grains [bioclasts -10%] and matrix [micrite – 70%, microspar – 4%, and clays & organics – trace], the sample was classified as limestone-mudstone. The crystal texture of the matrix is anhedral, while cement (11% of the total rock volume) shows subhedral to euhedral crystal texture. |
| Framework (Carbonate clasts, Bioclasts) | This lime-mudstone contains 94% of calcite. Other minerals include dolomite (5%), pyrite (1%), plus trace amounts of clays and organics. Framework grains are calcitic, and include mainly indistinct bioclasts (10%). |
| Detrital Grains & Other Non-Carbonate Grains | There are no detrital grains in this sample. |
| Matrix | Calcite-micrite is the main component of the matrix (70%), while clays and organics (associated with burrows) occur in trace amounts. Some of the micrite has re-crystallized to tightly packed mosaic microspar. The microspar accounts for about 4% of the total rock volume. |
| Pore Filling Cements | Calcite spar (10%), dolomite (4%), plus pyrite (trace) are the pore filling cements. |
| Replacement Minerals | Minor dolomite (4%) and pyrite (1%) also act as replacement minerals. |
| Porosity | There is no visible porosity in this sample. The RCA helium porosity that was measured on core plug is reported as 1.2%, while the gas permeability (affected by fractures) of the core sample is 11.5mD. The higher amounts of core porosity when compared with thin section porosity is due to microporosity of micrite. |

Annotated microphotographs of the thin section and SEM sample with descriptions are presented below.

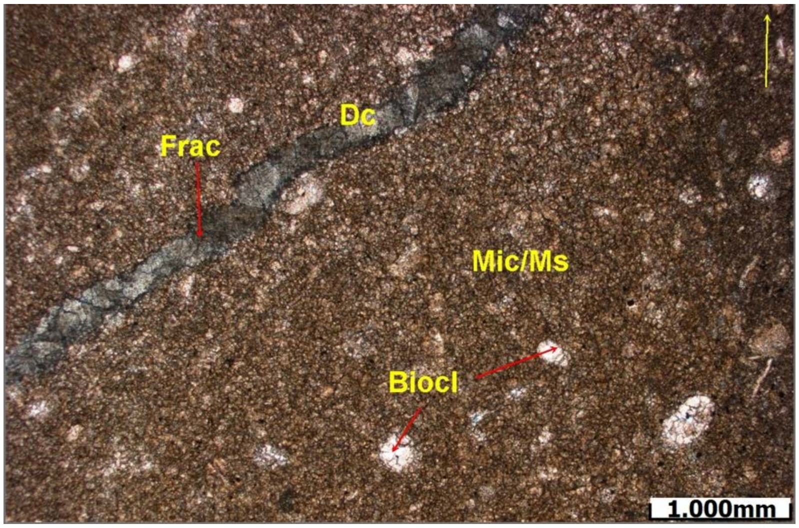


**Figure 6.1. Sample T16, 9000.40ft/2743.32m.** Low magnification image of the lime- mudstone shows the abundance of matrix that is mainly composed of micrite and minor amounts of microspar (Mic/Ms). Calcitic bioclasts fragments (Biocl) that are scattered throughout the matrix were impossible to identify due to their size and a high degree of recrystallization. Sub-vertical fracture is totally healed with medium crystalline dolomite (Frac; Dc). **x25ppl**

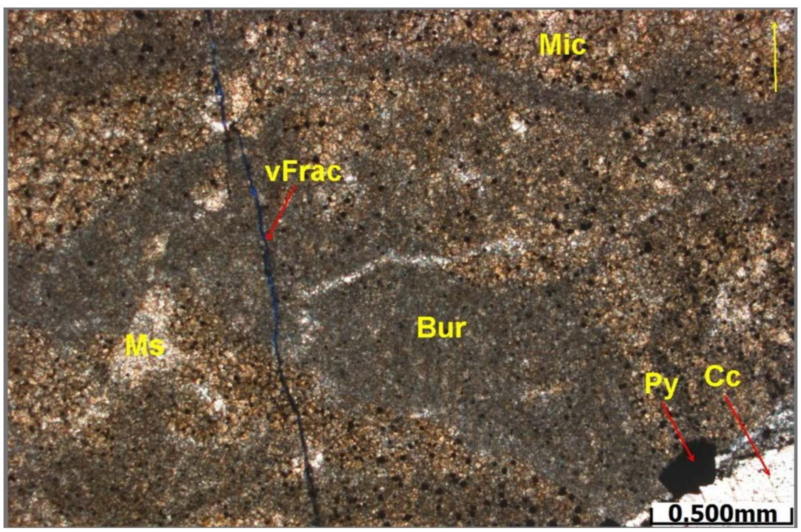


**Figure 6.2. Sample T16, 9000.40ft/2743.32m.** Moderate magnification image highlights the presence of horizontal burrows (Bur). The backfill of burrows is much darker than the surrounding micrite matrix (Mic) and microspar (Ms). This may suggest the presence of clays and organic material within the burrow fill. The vertical micro-fracture (vFrac) appears to be induced by the coring processes. In the lower right section of the image possible micro-vuggy pore has been filled with calcite spar (Cc). Aggregates of pyrite framboids and cubes partly replaces micrite (Py). **x50ppl**

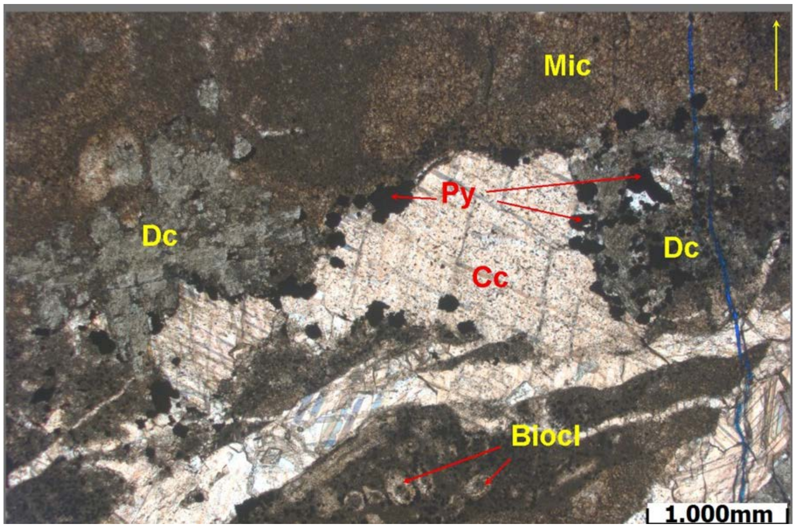


**Figure 6.3. Sample T16, 9000.40ft/2743.32m.** Low magnification image of the sample focuses on patches of replacement dolomite (Dc) that are locally replaced by pyrite framboids (Py). Large size void (middle) plus inclined fractures are totally filled with calcite spar (Cc). Pyrite framboids have also accumulated along the void/fracture. Micrite matrix (Mic) contains occasional indistinct bioclast fragments (Biocl). The sample appears tight. **x25ppl**

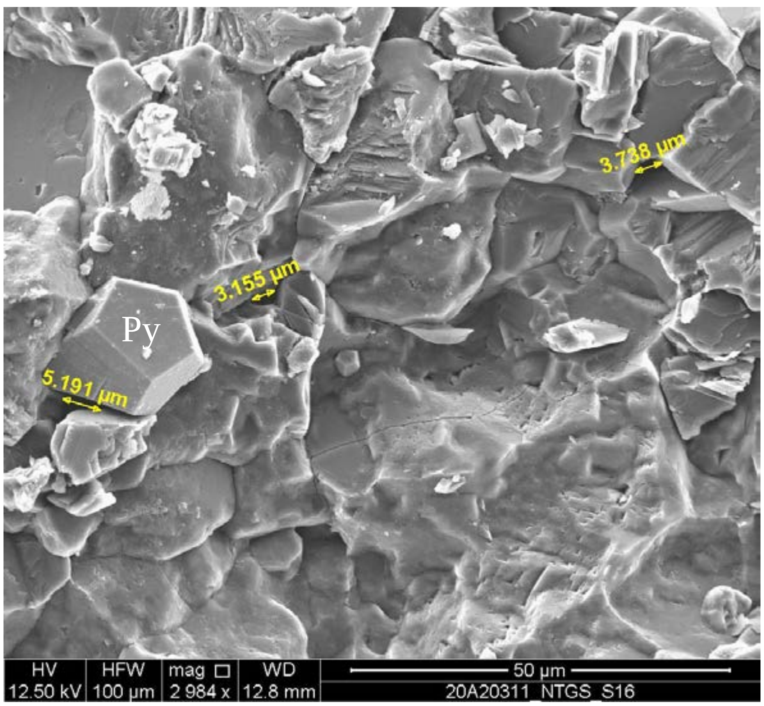


**Figure 6.4. Sample S16, 9000.40ft/2743.32m.** Moderate magnification scanning electron microscope (SEM) image showing microporosity (<5µm) associated with calcite micrite which comprises the matrix. Py: pyrite. **x2984**

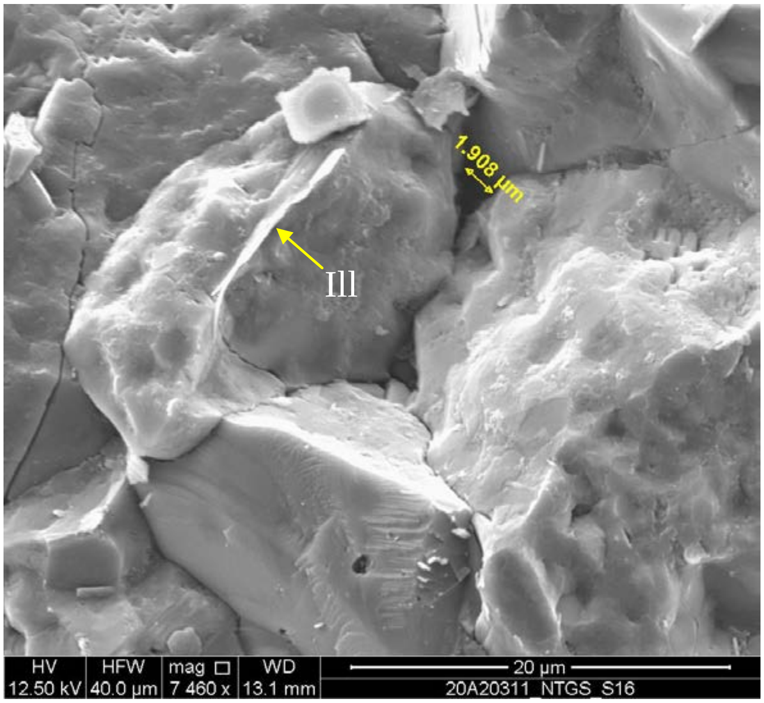


**Figure 6.5. Sample S16, 9000.40ft/2743.32m.** High magnification scanning electron microscope (SEM) image showing an open micropore between calcite crystallites. An illite (Ill) ribbon is loosely adhered to a crystal surface in this view. **x7460**

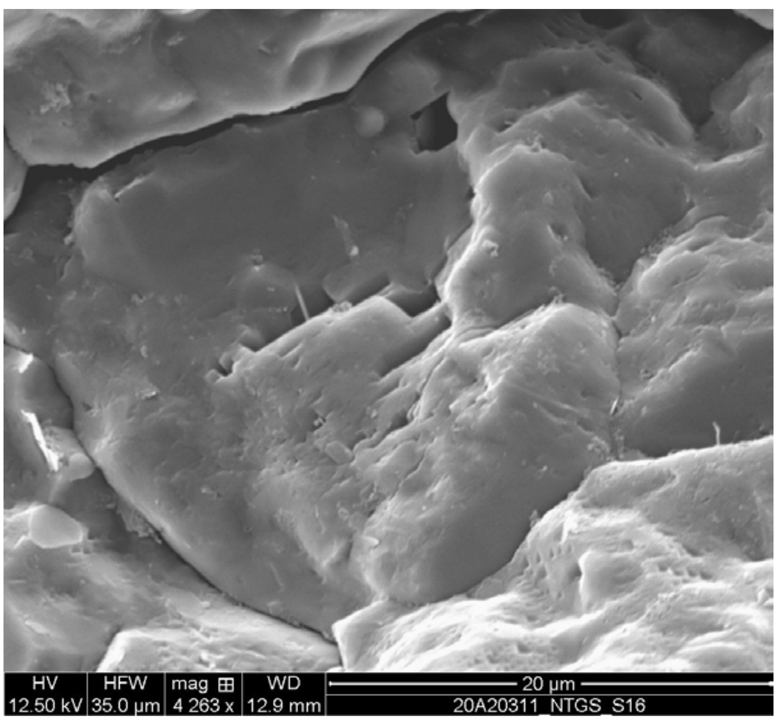


**Figure 6.6. Sample S16, 9000.40ft/2743.32m.** High magnification scanning electron microscope (SEM) image showing intra- and inter-crystalline micropores associated with the micritic matrix. **x4263**

## Sample T15/ S15/ P7, 9006.00ft/2745.03m

| | | | |
|---|---|---|---|
| **Well Name** | B.A. Texaco Arrowhead B-76 | **Location** | 300/B-76-6030-12245/0 |
| **Sample Type** | Thin section/SEM grain mount from a core sample | **Depth (m)** | 9006.00ft/2745.03m |
| **Stratigraphic Unit** | Nahanni Formation | **Reservoir Quality** | Poor |
| **Classification** | Limestone (Wackestone-Mudstone) | **Stain type** | ½ Dual carbonate stain |

**MINERALOGY**

| | Total bulk mineralogy | | | | | |
|---|---|---|---|---|---|---|
| Thin Section Point counting (%) | Calcite | Dolomite | Quartz | Pyrite | Clays & organics | |
| | 88 | 10 | TR | 1 | 1 | |
| | Framework, Matrix, Cement, and Replacement | | | | | |
| | Carbonate clasts | Bioclasts | Detrital grains | Matrix | Pore filling cement | Replacement |
| | - | 37 | TR | 42 | 15 | 6 |

**ADDITIONAL FEATURES and OTHER COMMENTS**

| | |
|---|---|
| **Depositional** | The sample is massive with no evident sedimentary structures. There are a few coarse crystalline dolomite and calcite spar healed sub-vertical fractures, and vertical low amplitude stylolites. Both fractures and stylolites have most likely formed during burial diagenesis (mechanical and chemical compaction of the sediment). |
| **Textures** | Based on the mineralogy and proportion between total bioclasts (37%) and matrix (42%), the sample was classified as limestone-wackestone to mudstone. For the matrix, the crystal texture has been determined as anhedral, while cement (5%) shows subhedral to euhedral crystal texture. Note that some of the micritic matrix has recrystallized into mosaic micro- or pseudospar (5%). |
| **Framework (Carbonate clasts, Bioclasts)** | The framework builders of this sample include indistinct bioclast fragments (20%), plus minor mollusks (5%), brachiopod (5%), ostracodes (5%), plus crinoids (2%). Note that the highly fragmented indistinct bioclast fragments have been point counted as a part of the matrix of this sample. |
| **Detrital Grains & Other Non-Carbonate Grains** | There is a trace amounts of detrital quartz grains that are randomly distributed through the matrix. |
| **Matrix** | The matrix consists of calcite micrite (36%), microspar (5%), plus clays and organics (1%). |
| **Pore Filling Cements** | Pore filling cement include calcite spar (10%), coarse crystalline dolomite (5%), plus trace pyrite. |
| **Replacement Minerals** | Dolomite locally acts as a replacement mineral (5%). Some of the pyrite replaces micrite, and appears to be incorporated (together with organic matter) into stylolitized laminae. |
| **Porosity** | There is no visible porosity in this sample. The RCA helium porosity that was measured on core plug is reported as 1.1%, while the gas permeability of the core sample is 0.13mD. The higher amounts of core porosity when compared with thin section porosity is due to microporosity of micrite. |

Annotated thin section and SEM microphotographs of the sample with descriptions follow below.

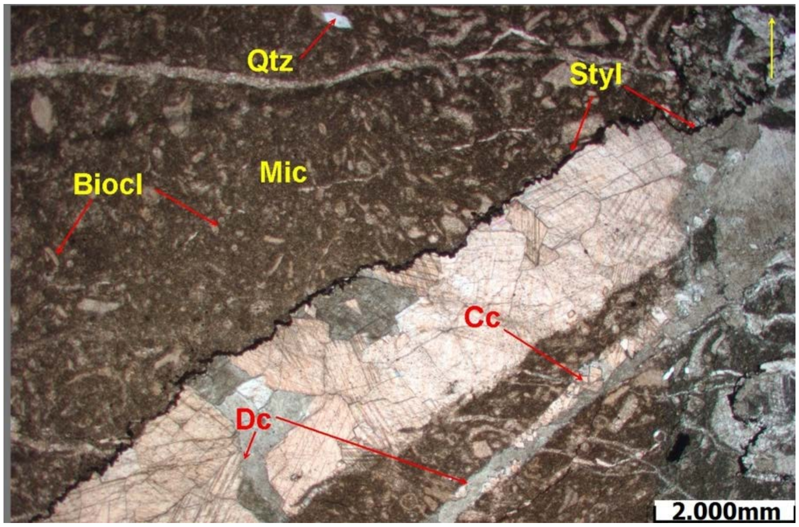


**Figure 7.1. Sample T15, 9006.00ft/2745.03m.** Low magnification overview of the wackestone-mudstone limestone focuses on inclined fractures that have been filled by coarse crystalline dolomite (Dc) followed by calcite spar (Cc). Note low amplitude stylolite (Styl) that outline the fracture. Abundant micritic matrix (Mic) contains fair amounts of highly fragmented indistinct bioclast fragments (Biocl). Rare detrital quartz grains (Qtz) were also spotted scattered throughout the matrix. Some of these grains have euhedral overgrowths. **x12.5ppl**

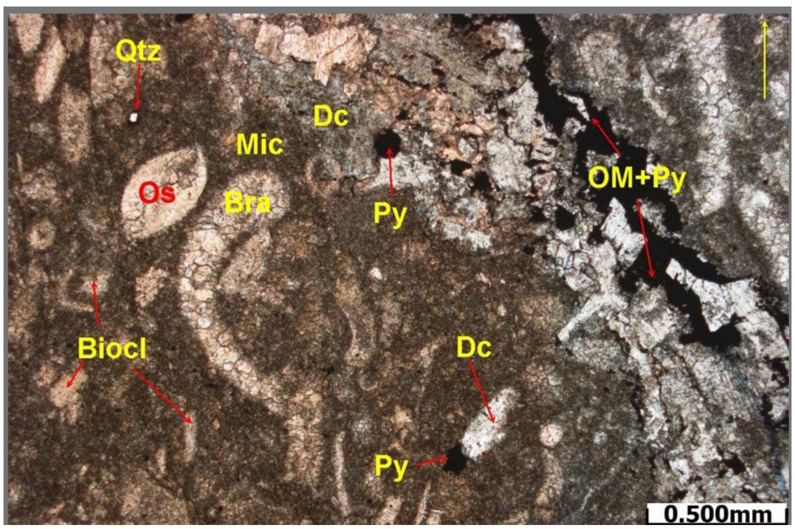


**Figure 7.2. Sample T15, 9006.00ft/2745.03m.** Moderate magnification image of the sample was taken on the border between stained (left) and unstained (right) portion of the thin section. The bioclast observed in this image include ostracode (Os), brachiopod (Bra), and indistinct bioclast fragments (Biocl). Detrital grains in this image are represented by quartz silt (Qtz). Note that some of the bioclasts have been cemented/replaced with dolomite (Dc- bottom). Remnants of replacement dolomite shows as grey-brown patches (upper-centre). Pyrite aggregates locally replace micrite (Py) and dolomite cement. Finely disseminated pyrite framboids are also associated with organic matter that fills low amplitude stylolites (OM+Py). **x50ppl**

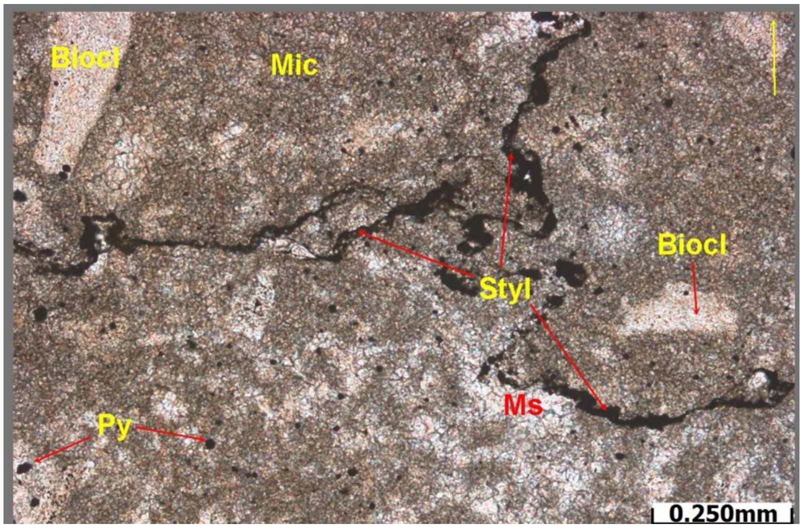


**Figure 7.3. Sample T15, 9006.00ft/2745.03m.** High magnification image focuses the presence stylolitized laminae (Styl) that cut through this sample. Note that the orientation of stylolites is both horizontal and vertical. The stylolites are marked by concentration of insoluble material (organic matter) along their irregular surface. Rare recrystallized indistinct bioclasts fragments (Biocl) are the framework builders. Micrite matrix (Mic) has been locally recrystallized to a mosaic microspar (MS). Pyrite framboids (Py) locally replace micrite. There is no visible porosity in this sample. **x100ppl**

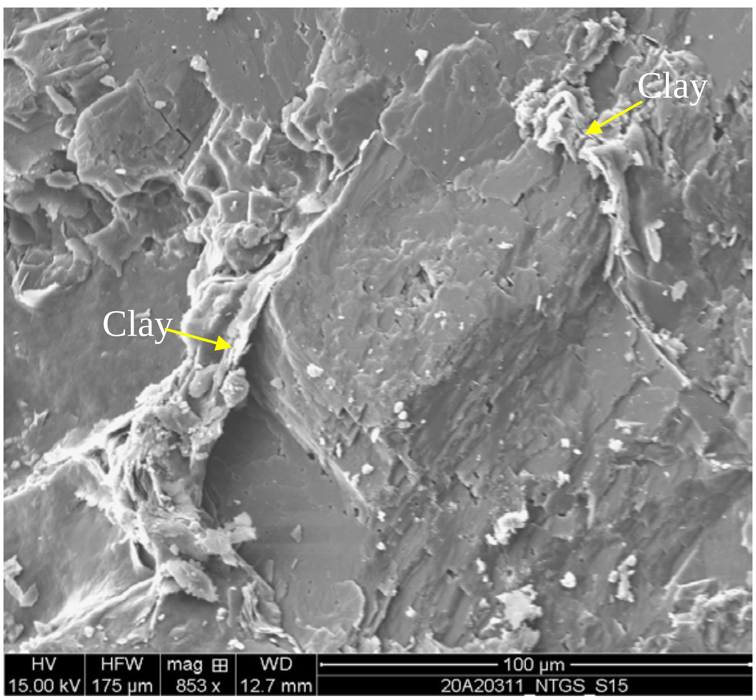


**Figure 7.4. Sample S15, 9006.00ft/2745.03m.** Low magnification scanning electron microscope (SEM) image showing interstitial platy clay minerals (Clay) or mica flakes. **x853**

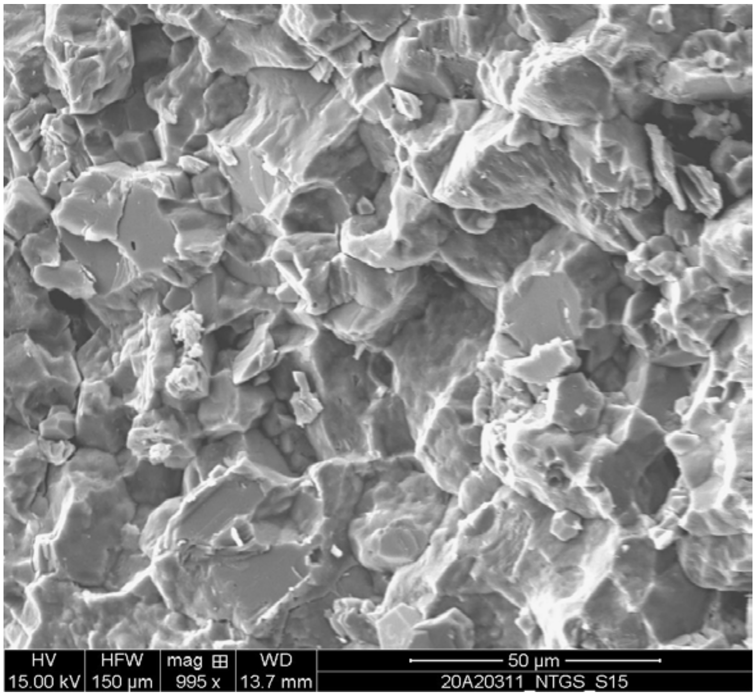


**Figure 7.5. Sample S15, 9006.00ft/2745.03m.** Low magnification scanning electron microscope (SEM) image of calcite micrite. Porosity is poor within this view. **x995**

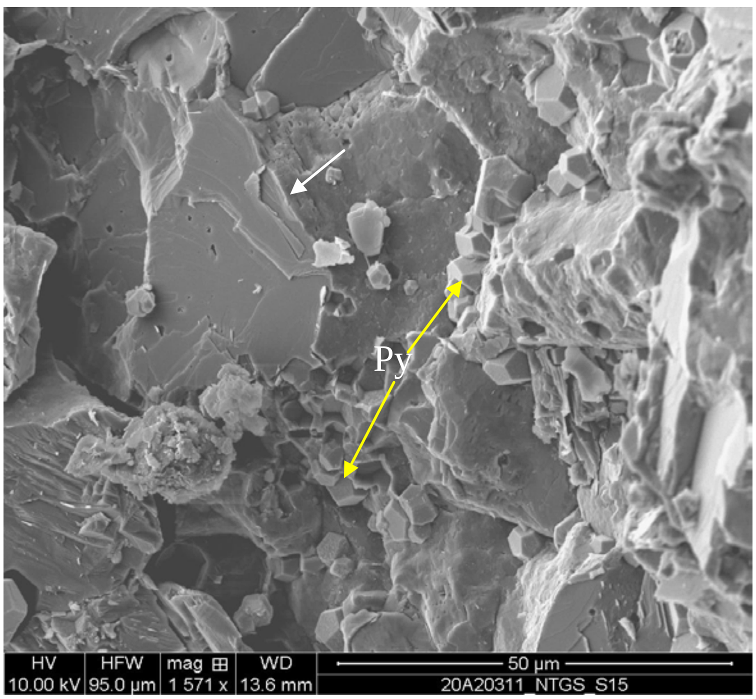


**Figure 7.6. Sample S15, 9006.00ft/2745.03m.** Moderate magnification scanning electron microscope (SEM) image showing clusters of pyrite (Py) dodecahedrons. The surrounding mineralogy shows tightly interlocking crystal boundaries (white arrow). **x1571**

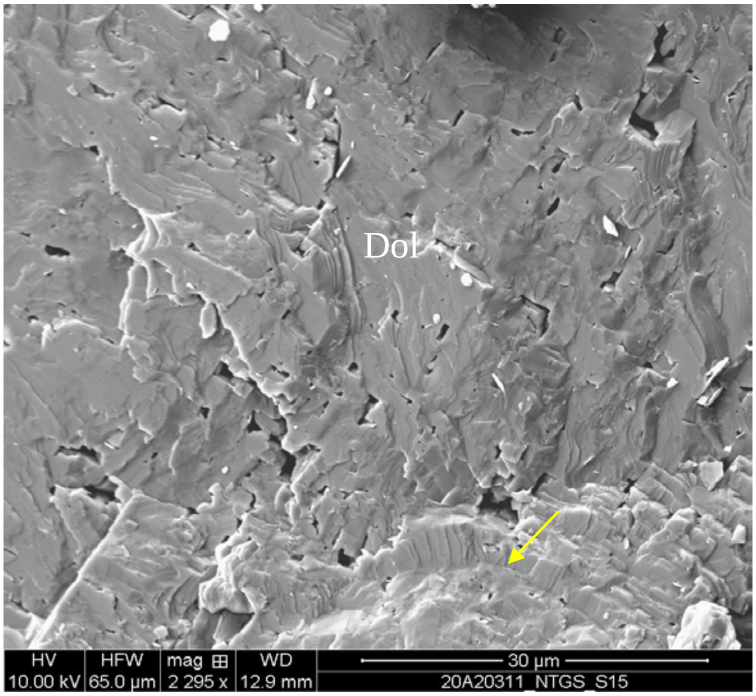


**Figure 7.7. Sample S15, 9006.00ft/2745.03m.** Moderate magnification scanning electron microscope (SEM) image of scattered micropores (<5µm) associated with dolomite cement. Crystal growth patterns outline the surface of a grain/bioclast (yellow arrow). **x2295**

## SUMMARY OF PORE SYSTEM, MAIN POROSITY CONTROLS AND RESERVOIR QUALITY

The reservoir quality of sediments is modified by diagenetic processes. Some diagenetic processes are directly related to the physical nature of the sediment, and can be directly related to sedimentation patterns. Other diagenetic processes involve the interaction of sediment with flowing interstitial water. Diagenetic features observed at this location include: onset of compaction, micritization of framework grains, dolomitization, dissolution of dolomite and possible un-dolomitized calcite grains, cementation of pores (coarse crystalline dolomite), partial replacement of dolomite cements with late calcite spar and pyrite, pressure solution (stylolites), authigenic silica replacements/cement, and pyrobitumen. Dolomitization is a diagenetic process that leads to dissolution of calcium carbonate and precipitation of dolomite. Dolomitization can change the rock fabric and petrophysical properties of the precursor limestone, because dolomite crystals are commonly larger than the replaced limestone particles. Dolomite cement occurs as euhedral usually coarse to very coarse crystalline rhombohedral cement that occludes micro-vugs and intercrystalline pores. The pervasive replacement dolomitization is the main diagenetic feature observed in dolostone samples. Diagenetic features developed prior to dolomitization have mostly been obliterated during the pervasive dolomitization. Some un-dolomitized calcite allochems were partly dissolved and dissolution pores and/or micro-vugs were filled with dolomite cement, megaquartz (see Figure 4.3), followed by pyrobitumen. Dolomite cement systematically grows on dolomite crystal faces, reducing reservoir quality. Chemical compaction also occurred post primary dolomitization. Chemical compaction is evidenced through pressure solution features like micro-stylolites. Insoluble bituminous organic matter and possible clays are found along these micro-stylolites. All the diagenetic features are not necessarily present in every sample.

### <u>Nahanni Formation</u>

A total of seven samples were recovered from the Nahanni Formation at the B.A. Texaco Arrowhead B-76 300/B-76-6030-12245/0 location. Samples T20, T19, T16, and T15 are limestones, while the other three samples (T21, T18, and T17) are dolostones.

Limestone samples

Based on the original texture of a rock, the samples were classified as grainstone (T20), wackestone (T19), mudstone (T16) and wackestone-mudstone (T15). There is no visible porosity in these four samples. The main porosity plugging factors for wackestone, mudstone, and wackestone-mudstone samples is the abundance of calcite micrite, which has locally recrystallized into tight mosaic microspar, plus the cementation (mainly of natural fractures) by calcite spar, coarse crystalline dolomite, plus trace pyrite. In the grainstone sample T20, the compaction (both mechanical and chemical), followed by the precipitation of syntaxial overgrowths on the crinoids plays the main role in destruction of the primary interparticle porosity.

Reservoir quality for these the wackestone, mudstone, and wackestone-mudstone samples is mainly controlled by depositional environment (i.e. abundance and distribution of lime-mud, crystal and grain size of the framework builders) and to lesser extent by diagenesis (i.e. mineral diagenesis, recrystallization of micrite to microspar, compaction, and cementation). Reservoir quality is considered to be poor for these three samples.

For the limestone-grainstone sample, the reservoir potential is almost equally controlled by depositional environment (i.e. abundance of the bioclasts) and by diagenetic events (i.e. mechanical and chemical compaction, precipitation of the framework sustaining cements such as syntaxial overgrowths, residual hydrocarbon, etc.). Reservoir quality of the grainstone is also considered to be poor based on lack of visible porosity.

Dolostone

All three dolostone samples comprise primarily dolomite, plus insignificant amounts of calcite, quartz, pyrite, clays and organics, plus pyrobitumen. The visible porosity in these three samples include trace to minor micro-vuggy and intercrystalline pores. Note that the micro-vuggy porosity is only observed in samples T18 and T17, while sample T21 shows trace amounts of

intercrystalline pores. The porosity reducing factors include precipitation of calcite spar cement (de-dolomitization), authigenic quartz, pyrobitumen, and pyrite.
Reservoir quality is controlled mainly by diagenetic events (i.e. dolomitization, dissolution, compaction, cementation [mostly euhedral dolomite] and pyrobitumen) and to a lesser extent the depositional environment (i.e. the original carbonate texture influences dolomite crystal size which correlates to the size and efficiency of the intercrystalline and micro-vuggy pores). Reservoir quality for the three dolostone samples is assessed as poor.

The following table summarizes the most important factors that control the reservoir quality of the seven samples recovered from the B.A. Texaco Arrowhead B-76 300/B-76-6030-12245/0 location. Note that the reservoir quality of these samples is accessed only based on the thin section petrology.

## NAHANNI Formation

| Sample ID | Depth (ft & m) | Total Micrite (%) | Total Cement/ Replacement (%) | Total Porosity (%) | | | | | | Main Porosity controlling factors (*) | RQ(*) |
|---|---|---|---|---|---|---|---|---|---|---|---|
| | | | | IP | Int. | Ixl | Mv | Fr | M | | |
| **Location: B.A. Texaco Arrowhead B-76 300/B-76-6030-12245/0** | | | | | | | | | | | |
| T21 | 8923.50ft 2719.88m | - | 97 | - | - | TR | - | - | - | Mic; Dol; Com; Cc; C; OM; Qc; Py | P |
| T20 | 8927.00ft 2720.95m | 2 | TR | - | - | - | - | - | - | Com; Ov; Mic; C; S; OM; Py | P |
| T19 | 8946.30ft 2726.83m | 39 | 1 | - | - | - | - | - | - | Mic; Cc; Ms; Com; Py; C; Qc | P |
| T18 | 8963.25ft 2732.00m | - | 100 | - | - | TR | TR | - | - | Mic; Dol; Py; OM; Qc; Com; Dis | P |
| T17 | 8988.20ft 2739.60m | - | 100 | - | - | 1 | 3 | - | - | Mic; Dol; Qc; Com; Dis; OM; Cc; Py; C | P |

| | | | | | | | | | | | |
|---|---|---|---|---|---|---|---|---|---|---|---|
| T16 | 9000.40ft 2743.32m | 74 | 16 | - | - | - | - | - | - | Mic; Cc; Dol; Ms; Dc; Py; C | P |
| T15 | 9006.00ft 2745.03m | 41 | 21 | - | - | - | - | - | - | Mic; Ms; Dc; Dol; C; Py | P |

**Porosity value (%):** **IP** – interparticle porosity; **Int** – intraparticle; **Ixl** – intercrystalline; **Mv** – micro-vuggy; **Fr** – fracture porosity; **M** – micro-intercrystalline porosity
**Main Porosity controlling factors:** **Com –** compaction (mechanical and chemical)**; Dol** – dolomitization; M**ic** – micrite (calcite or dolomite) and/or micritization; **Ms –** micro- and/or pseudospar; **Cc** – calcite cement (druse and spar); **Dc** – dolomite cement**; C** – clays and organics; **Qc** – quartz/chert cement; **Ov** – crinoid overgrowths; P**y** – pyrite (replacement and/or cement); **OM** – organic matter/pyrobitumen; **Dis** – dissolution; **F** – fabric: [**CC** – concavo-convex orthochem contacts; **S** – sutured orthochem contacts]
**RQ (*) - reservoir quality:** **VP –** very poor; **P –** poor; **M –** moderate; **G** - good

Reservoir problems for the samples recovered from the Nahanni Formation at the B.A. Texaco Arrowhead B-76 300/B-76-6030-12245/0 location may include the following: **(1)** rare and small sizes of intercrystalline and micro-vuggy pores, plus overall poor interconnectivity between pores could restrict the flow of hydrocarbons, **(2)** hydrochloric acid (HCl) treatment of this reservoir has the potential to loosen carbonate fines (calcite micrite) that could migrate and block pore throats, plus cause fabric collapse, **(3)** the sensitivity of calcium carbonate to hydrofluoric acid (HF) in regard to precipitation of calcium fluoride scales, (4) Pore lining pyrobitumen (especially in dolostone samples) may react with hydrochloric acid (HCl) to create sludges or viscous emulsions, which can restrict permeability potential. Both sludges and emulsions may be removed by using appropriate surfactants (surface active agents), which reduce interfacial and surface tension and result in a more miscible mixture of oil and water (acid). Any drilling, completion or workover must ensure the fluid acid compatibility with the formation pyrobitumen.

## Comments in regards to the Routine Core Analysis vs Thin Section point counted porosity

Porosity and permeability results derived from the Routine Core Analysis (RCA) can be found in the Petrographic Summary Tables 1 under the header 'Petrophysical Results'. The information regarding routine porosity and permeability are presented only to compare different methods that could be used in the assessment of reservoir quality, plus to see what could possibly affect the results. The table below shows the RCA samples, depth interval that they represent, helium porosity (Φ – %), and permeability ($K_{max}$), plus point counted porosity. Note that samples T21, T22, and T19 were not analyzed by the RCA.

| **Sample ID** | **Depth (ft & m)** | **RCA results** | | **TS Porosity Φ(%)** | **Rock Classification** |
|---|---|---|---|---|---|
| | | **Φ (%)** | **$K_{max}$ (mD)** | | |
| | | | | | |
| **Nahanni Formation** | | | | | |
| T21 | 8923.50ft 2719.88m | NA | NA | **TR** | Dolostone |
| T20 | 8927.00ft 2720.95m | NA | NA | Nil | Limestone (Grainstone) |
| T19 | 8946.30ft 2726.83m | NA | NA | Nil | Limestone (Wackestone) |
| T18 | 8963.25ft 2732.00m | 1.0 | 5.56* | TR | Dolostone |
| T17 | 8988.20ft 2739.60m | 3.1 | 42.0* | 4 | Dolostone |
| T16 | 9000.40ft 2743.32m | 1.2 | 11.5* | Nil | Limestone (Mudstone) |
| T15 | 9006.00ft 2745.03m | 1.1 | 0.13 | Nil | Limestone (Wackestone-Mudstone) |

**RCA – Routine Core Analysis; TS – Thin section (*) Permeability measurement affected by fractures**

The porosity calculated using RCA is higher when compared to the thin section point counting technique. The exception is the dolostone sample T17, where the thin section porosity is slightly higher than the helium porosity. The limestone samples of the Nahanni Formation comprise abundant amounts of micrite within the matrix, plus some of the allochems are also micritic. It should be noted that the Routine Core Analyses measure both effective (visible) and non-effective porosity (microporosity) associated with micrite, and micritized framework grains. On the other hand the thin section petrology only point counts the visible porosity. In the study samples, an abundance of microporosity is reflected by difference in measured core porosity. To summarize, the difference between thin section and core analysis is partially due to non-visible microporosity, which is associated with micrite, carbonate fines and microporous framework builders, the heterogeneity of core and thin section samples (heterogeneous distribution of cements) and the difference in dimension (aspect ratio) of thin section and core samples[2].

[2] During the thin section examination a two-dimensional representative area is analyzed, whereas petrophysical core analysis reflects the three-dimensional pore volume.

## REFERENCES

Folk, R. L. (1974), Petrology of Sedimentary Rocks. Hemphills, Austin, Texas, USA.

Scholle, P.A. and Ulmer-Scholle, D.S. 2006. A Color Guide to the Petrography of Carbonate Rocks: Grains, Textures, Porosity, Diagenesis. AAPG Memoir 77. American Association of Petroleum Geologists, Tulsa, O.K.

Welton, J.E. 2003. SEM Petrology Atlas. Methods in Exploration Series No. 4. American Association of Petroleum Geologists, Tulsa, O.K.

# DATA TABLES

# Table 1
## Petrographic Summary of Seven Samples recovered from the Nahanni Formation at the B.A. Texaco Arrowhead B-76 300/B-76-6030-12245/0 Location

| **Sample ID** | | **T21** | **T20** | **T19** | **T18** | **T17** | **T16** |
|---|---|---|---|---|---|---|---|
| **Depth (ft)** | | **8923.50** | **8927.00** | **8946.30** | **8963.25** | **8988.20** | **9000.40** |
| **Rock Type** | | **DS** | **LS** | **LS** | **DS** | **DS** | **LS** |
| **Mineralogy** | *Calcite* | 2 | 97 | 99 | TR | 1 | 94 |
| | *Dolomite* | 96 | - | - | 97 | 93 | 5 |
| | *Anhydrite* | - | - | - | - | - | - |
| | *Quartz/Chert* | TR | - | TR | TR | 4 | - |
| | *Phosphate* | - | - | TR | - | - | - |
| | *Pyrite and Heavy Minerals* | TR | TR | 1 | 2 | TR | 1 |
| | *Pyrobitumen* | 1 | 1 | - | 1 | 2 | - |
| | *Clays & organics* | 1 | 2 | **TR** | - | TR | TR |
| **Total Rock Volume (%)** | | **100** | **100** | **100** | **100** | **100** | **100** |
| **Carbonate Clasts** | *Peloids* | - | - | - | - | - | - |
| | *Ooids* | - | - | - | - | - | - |
| | *Intraclasts/Oncolintes* | - | - | - | - | - | - |
| | ***Total:*** | **0** | **0** | **0** | **0** | **0** | **0** |
| **Bioclasts/Fauna** | *Mollusks* | - | - | 10 | - | - | - |
| | *Foraminifers* | - | - | - | - | - | - |
| | *Brachiopod (shell & spines)* | - | - | 5 | - | - | - |
| | *Bryozoa* | - | - | - | - | - | - |
| | *Corals* | - | 30 | - | - | - | - |
| | *Algae* | - | - | - | - | - | - |
| | *Echinoderms/Crinoids* | - | 45 | 25 | - | - | - |
| | *Trilobites* | - | - | - | - | - | - |
| | *Ostracodes* | - | - | 10 | - | - | - |
| | *Stromatoporoid* | - | 20 | - | - | - | - |
| | *Unidentified* | 2 | - | - | TR | - | 10 |
| | ***Total:*** | **2** | **95** | 50 | TR | **0** | **10** |
| **Detrital Grains and Other Non-Carbonate Grains** | *Quartz* | - | - | - | - | - | - |
| | *Chert* | - | - | - | - | - | - |
| | *Phosphate* | - | - | TR | - | - | - |
| | ***Total:*** | **0** | **0** | TR | **0** | **0** | **0** |
| **Matrix** | *Micrite (calcite or dolomite)* | - | 2 | 37 | - | - | 70 |
| | *Micro- and pseudospar* | - | | 2 | - | - | 4 |
| | *Clays & organics* | 1 | 2 | TR | - | TR | TR |
| | *Sutured allochems* | - | - | - | - | - | - |
| | ***Total:*** | **1** | 4 | 39 | **0** | TR | 74 |
| **Pore Filling Cement** | *Calcite Spar* | 2 | - | 10 | - | 1 | 10 |
| | *Calcite druse* | - | - | - | - | - | - |
| | *Dolomite* | - | - | - | TR | TR | 1 |
| | *Quartz/Chert* | TR | - | - | TR | 4 | - |
| | *Pyrite* | TR | - | - | 2 | TR | TR |
| | *Pyrobitumen* | 1 | 1 | - | 1 | 2 | - |
| | ***Total:*** | **3** | 1 | 10 | 3 | 7 | 11 |
| **Replacement** | *Calcite* | - | - | - | - | - | - |
| | *Dolomite* | 94 | - | - | 97 | 93 | 4 |
| | *Anhydrite* | - | - | - | - | - | - |
| | *Quartz/Chert* | - | - | TR | - | - | - |
| | *Pyrite* | TR | TR | 1 | - | TR | 1 |
| | ***Total:*** | **94** | **TR** | 1 | 97 | 93 | **5** |
| **Total Rock Volume (%)** | | **100** | **100** | **100** | **100** | **100** | **100** |
| **Crystal Texture (Matrix)** | | - | Anh | Anh | - | - | Anh |
| **Crystal Texture (Cement)** | | Sub-Euh | Sub-Euh | Euh | Sub-Euh | Sub-Euh | Sub-Euh |
| **Crystal Size (Dolomite)** | | VCxl | - | - | VCxl | VCxln | - |
| **Structure/Fabric** | | Styl | Styl, S | Frac | - | Fracs | Bur; fracs |
| **Ratio Matrix/Clasts (approximate)** | | - | 1:50 | 1:2 | - | NA | 7:1 |
| **Original Texture** | | - | GS | WS | - | - | MS |
| **Porosity (%)** | *Interparticle* | - | - | - | - | - | - |
| | *Intraparticle* | - | - | - | - | - | - |
| | *Intercrystalline* | TR | - | - | TR | 1 | - |
| | *Fracture* | - | - | - | - | - | - |
| | *Micro-Vuggy* | - | - | - | **TR** | **3** | - |
| | *Micro- intercrystalline pores* | - | - | - | - | - | - |
| | ***Total TS Porosity (%)*** | **TR** | **0** | **0** | **TR** | **4** | **0** |
| **Petrophysical Results** | *Core Porosity (%)* | **NA** | **NA** | **NA** | **1.00** | **3.10** | **1.20** |
| | *Core Permeability (mD)* | **NA** | **NA** | **NA** | **5.56*** | **42.0*** | **11.5*** |
| **Reservoir Quality** | | **Poor** | **Poor** | **Poor** | **Poor** | **Poor** | **Poor** |

# Table 1 (continued)
## Petrographic Summary of Seven Samples recovered from the Nahanni Formation at the B.A. Texaco Arrowhead B-76 300/B-76-6030-12245/0 Location

| | | | | | | | | |
|---|---|---|---|---|---|---|---|---|
| **Sample ID**<br>**Depth (ft)**<br>**Rock Type** | | **T15**<br>**9006.00**<br>**LS** | | | | | | |
| **Mineralogy** | *Calcite* | 88 | | | | | | |
| | *Dolomite* | 10 | | | | | | |
| | *Anhydrite* | - | | | | | | |
| | *Quartz/Chert* | TR | | | | | | |
| | *Phosphate* | - | | | | | | |
| | *Pyrite and Heavy Minerals* | 1 | | | | | | |
| | *Pyrobitumen* | - | | | | | | |
| | *Clays & organics* | 1 | | | | | | |
| **Total Rock Volume (%)** | | **100** | | | | | | |
| **Carbonate Clasts** | *Peloids* | - | | | | | | |
| | *Ooids* | - | | | | | | |
| | *Intraclasts/Oncolintes* | - | | | | | | |
| | ***Total:*** | **0** | | | | | | |
| **Bioclasts/Fauna** | *Mollusks* | 5 | | | | | | |
| | *Foraminifers* | - | | | | | | |
| | *Brachiopod (shell & spines)* | 5 | | | | | | |
| | *Bryozoa* | - | | | | | | |
| | *Corals* | - | | | | | | |
| | *Algal* | - | | | | | | |
| | *Echinoderms/Crinoids* | 2 | | | | | | |
| | *Trilobites* | - | | | | | | |
| | *Ostracodes* | 5 | | | | | | |
| | *Stromatoporoid* | | | | | | | |
| | *Unidentified* | 20 | | | | | | |
| | ***Total:*** | **37** | | | | | | |
| **Detrital Grains and Other Non-Carbonate Grains** | *Quartz* | TR | | | | | | |
| | *Chert* | - | | | | | | |
| | *Phosphate* | - | | | | | | |
| | ***Total:*** | **TR** | | | | | | |
| **Matrix** | *Micrite (calcite or dolomite)* | 36 | | | | | | |
| | *Micro- and pseudospar* | 5 | | | | | | |
| | *Clays & organics* | 1 | | | | | | |
| | *Sutured allochems* | - | | | | | | |
| | ***Total:*** | **42** | | | | | | |
| **Pore Filling Cement** | *Calcite Spar* | 10 | | | | | | |
| | *Calcite druse* | - | | | | | | |
| | *Dolomite* | 5 | | | | | | |
| | *Ferroan Dolomite* | - | | | | | | |
| | *Pyrite* | TR | | | | | | |
| | *Pyrobitumen* | - | | | | | | |
| | ***Total:*** | **15** | | | | | | |
| **Replacement** | *Calcite* | - | | | | | | |
| | *Dolomite* | 5 | | | | | | |
| | *Anhydrite* | - | | | | | | |
| | *Quartz/Chert* | - | | | | | | |
| | *Pyrite* | 1 | | | | | | |
| | ***Total:*** | **6** | | | | | | |
| **Total Rock Volume (%)** | | **100** | | | | | | |
| **Crystal Texture (Matrix)** | | Anh | | | | | | |
| **Crystal Texture (Cement)** | | Sub-Euh | | | | | | |
| **Structure/Fabric** | | Styl; fracs | | | | | | |
| **Ratio Matrix/Clasts (approximate)** | | 1:1 | | | | | | |
| **Original Texture** | | WS-MS | | | | | | |
| **Porosity** | *Interparticle* | - | | | | | | |
| | *Intraparticle* | - | | | | | | |
| | *Intercrystalline* | - | | | | | | |
| | *Fracture* | - | | | | | | |
| | *Micro-Vuggy* | - | | | | | | |
| | *Micro- intercrystalline pores* | - | | | | | | |
| | ***Total TS Porosity (%)*** | 0 | | | | | | |
| **Petrophysical Results** | *Core Porosity (%)* | **1.1** | | | | | | |
| | *Gas Permeability (mD)* | **0.13** | | | | | | |
| **Reservoir Quality** | | **Poor** | | | | | | |

# LIST OF ABBREVIATIONS (CARBONATES)

**SKELETAL GRAINS**

Bry - BRYOZOAN
Ech - ECHINODERMS
Bra - BRACHIOPODS
Os - OSTRACODS
Cal - CALCISPHERES
Moll - MOLLUSKS
Plcy - PELECYPODS
Biv - BIVALVES
For - FORAMINIFERA
Strom - STROMATOPOROIDS
Cor - CORALS
Ga - GASTROPODS
Biocl - BIOCLASTS

**OTHER GRAINS**

Pel - PELOIDS
Ooi - OOIDS

**ORIGINAL TEXTURE**

GS - GRAINSTONE
PS - PACKSTONE
WS - WACKESTONE
MS - MUDSTONE
FS - FLOATSTONE
RS - RUDSTONE

**CRYSTAL TEXTURE**

Euh - EUHEDRAL
Sub - SUBHEDRAL
Anh - ANHEDRAL

**CRYSTAL SIZE**

Cxl - COARSE CRYSTALLINE
Mxl - MEDIUM CRYSTALLINE
Fxl - FINE CRYSTALLINE
Vfxl - VERY FINE CRYSTALLINE

**CEMENT TYPES**

Syn - SYNTAXIAL OVERGROWTHS
Blo - BLOCKY
Poik - POIKILOTOPIC
Dru - DRUSY
SD - SADDLE DOLOMITE
Lath - ANHYDRITE LATHS
Grm - GROUNDMASS
Iso - ISOPACHOUS RIMS
Spa - SPARITE

**POROSITY TYPES**

Mixl - MICRO-INTERCRYSTALLINE
Ixl - INTERCRYSTALLINE
Mo - BIOMOLDIC
mV - MICROVUGGY
mF - MICROFRACTURE
IG - INTERGRANULAR
IP - INTERPARTICLE
INTRP - INTRAPARTICLE

**QUALITY**

G - GOOD
M - MODERATE
P - POOR

**Well Name:** **B.A. Texaco Arrowhead B-76**
**Well ID:** **300/B-76-6030-12245/0**
**NT WID #** **N222**

**Table 2**: Results of quantitative mineral analysis (relative weight %) of X-ray diffraction data for 5 (five) samples using Rietveld method

| Geology ID | Depth (ft) | Depth (m) | Core & Box # | NTGS Sample Type & # | **Calcite** | **Dolomite** | **Quartz** | **Plagioclase feldspar** | **Apatite** | **Pyrite** | **Total** |
|---|---|---|---|---|---|---|---|---|---|---|---|
| 1 | 8927.00 | 2720.95 | 3 & 5 of 14 L | T20,X39, S20 | 99.4 | 0.4 | 0.2 | | | | 100 |
| 2 | 8946.30 | 2726.83 | 3 & 10 of 14L | T19, X38, S19 | 98.7 | | 0.6 | | 0.4 | 0.3 | 100 |
| 3 | 8963.25 | 2732.00 | 4 & 1 of 13 R | T18, X37, S18, P11 | 3.0 | 96.0 | 0.3 | 0.5 | | 0.2 | 100 |
| 4 | 8988.20 | 2739.60 | 4 & 7 of 13 L | T17,X36, S17, P10 | 10.6 | 88.0 | 0.8 | 0.5 | | 0.1 | 100 |
| 5 | 8997.00 | 2742.29 | 4 & 10 of 13 R | X35, P9 | 95.7 | 2.4 | 1.9 | | | | 100 |

AGAT Laboratories